Three essays on equilibrium selection with coupled populations

Inauguraldissertation
zur Erlangung des akademischen Grades

Doctor rerum politicarum

eingereicht an der

Wirtschaftswissenschaftlichen Fakultät der
Heinrich Heine Universität Düsseldorf

von

Ismael Martínez Martínez
geboren am 3. April 1989 in Madrid (Spanien).

—

Rektorin der Heinrich Heine Universität Düsseldorf:
Univ.-Prof. Dr. Anja Steinbeck

Dekan der Wirtschaftswissenschaftlichen Fakultät:
Univ.-Prof. Dr. Justus Haucap

Erster Gutachter:
Univ.-Prof. Dr. Hans-Theo Normann
Heinrich Heine Universität Düsseldorf

Zweiter Gutachter:
Univ.-Prof. Dr. Alexander Rasch
Heinrich Heine Universität Düsseldorf

December 2016

"Theories are nets to catch what we call 'the world': to rationalize, to explain, and to master it. We endeavour to make the mesh ever finer and finer."

Karl Popper, in The Logic of Scientific Discovery (1935)

HEINRICH HEINE UNIVERSITÄT

Abstract

Wirtschaftswissenschaftliche Fakultät
Düsseldorf Institute for Competition Economics (DICE)

Doctor rerum politicarum

Three essays on equilibrium selection with coupled populations

by Ismael Martínez Martínez

Predictions of evolutionary game theory with regard to equilibrium selection generally depend on whether players interact within a single population or between two (or more) different populations. Standard one- and two-population models are the limit cases of a uniparametric family that combines intra- and intergroup interactions. This dissertation studies a setup that interpolates between both extremes with a coupling parameter κ. We analyze the bifurcation in the replicator dynamics of the coupled model applied to the hawk-dove game in Chapter 1. We identify three regions for equilibrium selection, one of which does not appear in basic one- and two-population models. We also design and conduct an innovative experiment in continuous time that widely confirms the theoretical predictions. Among some subtleties in the behavior of the system for intermediate values of κ, we observe a systematic bias in the share of hawk play in the mixed regime, and an upward shift in the critical value of κ for which polarizing behavior begins. We account for these effects by extending the model to consider perturbed best response dynamics in Chapter 2. Finally, Chapter 3 proposes a generalization of the original model to situations where the intra- and intergroup interactions can be any pair of different games defined by 2×2 payoff matrices. Replicator dynamics predicts a maximum of twenty-one possible scenarios for equilibrium selection. Motivated by the findings in Chapter 2, we introduce a model of perturbed best response dynamics which reduces these cases to only four behavioral families. This exhaustive analysis of the more general model with coupled populations paves the way for a further experimental agenda based on the predictions of Chapter 3 and the experiment in continuous time designed for Chapter 1.

Acknowledgements

I would like to thank all the people that helped me improve at both the academic and personal level at different stages of my doctoral studies, foremost,

my first supervisor, Hans,
because there is no successful dissertation without the right guidance;

my second supervisor, Alexander; my coauthor, Volker;

Hamid, Maria, and my family for their support during these three years.

—

Funding from the Düsseldorf Institute for Competition Economics is, of course, gratefully acknowledged.

Contents

Abstract **ii**

Acknowledgements **iii**

Contents **iv**

List of Figures **vi**

List of Tables **vii**

Preface **1**

Introduction **2**

1 Equilibrium selection with coupled populations in hawk-dove games: Theory and experiment in continuous time **5**

1.1 Introduction 6

1.2 Literature 9

1.3 Theory 10

1.4 Experiment 15

1.5 Results 17

1.6 Conclusion 22

Appendix - Proof of Proposition 1 23

2 Perturbed best response dynamics in a hawk-dove game 26
2.1 Introduction 27
2.2 PBR model 28
2.3 Experiment 31
2.4 Results 32
2.5 Discussion 34

3 A general model for 2×2 games with coupled populations 37
3.1 Introduction 38
3.2 Basic coupled model 39
3.3 Angular representation of games 40
3.4 Replicator dynamics 45
3.5 PBR dynamics 53
3.6 Scenarios of equilibrium predictions 55
3.7 Conclusion 60
Appendix A - Linear stability analysis 61
Appendix B - Additional tables 65

Conclusion 67

Experimental instructions 68

Bibliography 74

List of Figures

1.1 Population structures 10
1.2 Replicator dynamics 14
1.3 Experimental display 18
1.4 Experimental timelines 19
1.5 Aggregate results 20

2.1 Perturbed best response dynamics 30
2.2 Experimental results (I) 32
2.3 Experimental results (II) 34

3.1 Angular classification of 2×2 games 42
3.2 Critical values of coupling 48
3.3 Regions of predictions in the space of angular parameters 50
3.4 Bifurcations predicted by replicator dynamics 52
3.5 Solutions with PBR dynamics 54
3.6 Coupling conditions for the existence of hybrid and mixed states . . 62

List of Tables

1.1 Fixed points' location (replicator dynamics) 13
1.2 Sequence of treatments in each session 16

3.1 Baseline equilibria: static games and basic population structures . . 44
3.2 Fixed points of replicator dynamics 46
3.3 Critical values of κ 47
3.4 Bifurcation scenarios 65
3.5 Angular values used in Figure 3.4 66
3.6 Payoff matrices used in Figure 3.5 66

Preface

This dissertation is a result of the three years spent as a doctoral student at the Düsseldorf Institute for Competition Economics under the supervision of Prof. Dr. Hans-Theo Normann and Prof. Dr. Alexander Rasch. My main research foci have been on the application of mathematical and experimental techniques to study patterns in human decision-making, with special attention to strategic interactions in dynamic environments. During this period of time, I have worked simultaneously in two different areas: the analysis of equilibrium selection in evolutionary games with coupled populations, and the development of models for decision-making dynamics within a non-classical probability framework.

The following chapters deal with the first topic as a concise monograph. Therefore, I only enumerate here the accomplishments in the field of non-classical models for decision-making and refer the interested reader to the peer-reviewed publications. Martínez-Martínez, (2014), published in the *Journal of Mathematical Psychology*, explains some departures from perfect rationality with concepts of superposition and entanglement between actions and beliefs. Lambert-Mogiliansky and Martínez-Martínez, (2015), published as a chapter in *Lecture Notes in Computer Science*, proposes a model for games with contextual preferences. Martínez-Martínez and Sánchez-Burillo, (2016), published in *Scientific Reports*, applies the general framework of quantum stochastic walks on networks for decision-making and accounts for different behavioral traits, including violations of the sure thing principle. Denolf et al., (in press) in the *Journal of Mathematical Psychology*, explains the experimental findings by Blanco et al., (2014) with the notion of complementarity between observed preferences and beliefs of the subjects; their interaction is a natural consequence of the measurement of two incompatible observables.

Introduction

Equilibrium selection is a fundamental issue in the application of game theoretical models; especially because normal form games usually show multiple Nash equilibria (Harsanyi and Selten, 1988). Evolutionary and learning dynamics play a major role in the study of this fundamental question (Friedman, 1991). Simple strategic models are enriched with information about the structure of the population, among other aspects. A renowned example is the distinction made by evolutionary game theory when an interaction is described as a one- or a two-population game (Cressman, 2003; Weibull, 1995). The first model favors symmetric configurations, while the second allows for specialization among groups. As argued in the following chapters, such sharp distinction between interactions within a group or between groups establishes an important restriction: both models require a large degree of isolation between agents that belong to a different or the same group, in one way or another.

We relax this constraint and analyze what happens when both interactions overlap. This dissertation provides an exhaustive study of the dynamics and the equilibrium selection with coupled populations. The manuscript follows an incremental approach and aims for a self-contained and concise exposition. The first chapter develops the core ideas with a model of coupled replicator dynamics applied to the case of hawk-dove games, and with a novel experiment in continuous time. The next two chapters extend this study in two complementary directions: first, we consider deviations from the best response paradigm to explain the behavioral subtleties observed in the experiment; and second, we generalize the original model to allow the intra- and intergroup interactions to be any pair of symmetric two-strategy games defined with 2×2 payoff matrices, Π_A and Π_B.

Chapter 1 is published in the *Journal of Economic Theory* (Benndorf et al., 2016). We first provide the basic motivations for the study of overlapping intra- and

intergroup interactions and conduct a thorough analysis of the model for hawk-dove games ($\Pi_A = \Pi_B$), both theoretically and with experiments in continuous time. We propose the model for coupled replicator dynamics with the introduction of the coupling parameter $\kappa \in [0, 1]$ that interpolates linearly between the one- and two-population models when $\kappa = 0$ and $\kappa = 1$, respectively. The theoretical analysis predicts three regions with different stable equilibria. For any level of κ below a threshold $\kappa_m^* = \frac{1}{2}$ the predictions is a non-degenerate mixed equilibrium as in the one-population setting. For $\kappa > v/c > \frac{1}{2}$ (where v and c are the value and cost of the conflict in the hawk-dove game, respectively), pure play emerges. The intermediate regime $\kappa \in (\kappa_m^*, \kappa_p^*)$ shows a qualitatively novel prediction where one population coordinates on a pure strategy and the second one randomizes with a pure mixture of hawks and doves. This situation does not occur with standard one- and two-population models, or in the basic static setting. These predictions can be understood as a sign that the one-population case extends with much overlap to the second population; while the range of coupling where pure equilibria can be sustained is more moderate. Overall, the two extreme one and two-population cases are robust with respect to moderate perturbations. The experiment in continuous time confirms the predictions qualitatively, and especially with regard to the evolution of the separation observed in the play by both populations. We find mixed behavior in the predicted regime and also the transition toward a sound separation for greater values of κ. But we also observe a considerable level of heterogeneity across sessions in the location of the splitting point (coupling level for which the populations split into two groups of mostly hawks or doves).

Chapter 2 is motivated by these final observations in Chapter 1. On the one hand, replicator dynamics predicts symmetric mixed play with $\frac{2}{3}$ of hawk play for $\kappa < \frac{1}{2}$, and a sudden bifurcation is expected at $\kappa = \frac{1}{2}$ such that one population plays pure hawk and the other plays mixed strategy with $\frac{1}{3}$ of hawk. Separation increases monotonically on κ in the interval $[\frac{1}{2}, \frac{2}{3}]$ and the system is totally polarized for $\kappa > \frac{2}{3}$. On the other hand, a perturbed best response model applied to our experimental setting makes two more refined predictions by introducing behavioral noise (logit function) in the selection of actions with finite λ, in line with the minor subtleties observed in Chapter 1. The share of hawk choices in the symmetric mixed equilibrium can be lower than $\frac{2}{3}$; and perturbed best response dynamics implies that the impact of the polarizing forces on the behavior of the system is weaker

than suggested by replicator dynamics. Both results are positive given our data set.

Chapter 3 revisits the theoretical model introduced in Chapter 1 for the special case of hawk-dove games and generalizes the benchmark of coupled interactions to any pair of 2×2 symmetric payoff matrices (in general, $\Pi_A \neq \Pi_B$). We show how only three parameters are sufficient to cast any possible overlap of interactions of this kind, and relate a derivation of the coupling parameter κ to the fundamental scaling parameters of the payoff matrices in angular notation. As a result, we obtain a total of twenty-one possible bifurcations with replicator dynamics, the majority of them presenting more intricate predictions regarding the regimes with intermediate levels of coupling than those observed in Chapter 1. Following from the evidence accumulated in Chapter 2 about how human behavior in the lab can be fairly accounted for with the introduction of noise in the perturbed best response dynamics, we are able to regroup these scenarios to a set of four families of behavioral predictions.

Chapter 1

Equilibrium selection with coupled populations in hawk-dove games☆

Theory and experiment in continuous time

Summary of the chapter

Standard one- and two-population models for evolutionary games are the limit cases of a uniparametric family combining intra- and inter-group interactions. Our setup interpolates between both extremes with a coupling parameter κ. For the example of the hawk-dove game, we analyze the replicator dynamics of the coupled model. We confirm the existence of a bifurcation in the dynamics of the system and identify three regions for equilibrium selection, one of which does not appear in common one- and two-population models. We also design a continuous-time experiment, exploring the dynamics and the equilibrium selection. The data largely confirm the theory.

☆This chapter is published in the *Journal of Economic Theory*, 165 (2016) 472–486, co-authored with Volker Benndorf and Hans-Theo Normann.

1.1 Introduction

Evolutionary game theory makes an important distinction as to whether players interact within a single population or between two (or more) disjunct populations (Cressman, 2003; Friedman, 1991; Weibull, 1995). When matched with opponents in a single population, players earn the expected payoff as if playing against the aggregate strategy of their own population, so only symmetric strategies can survive. With a two-population matching, each member of the group of, say, row players is matched against a rival from the group of column players. Here, polarization in behavior can occur and the populations may specialize in different strategies. The same evolutionary forces can thus imply qualitatively different results, so the distinction of single- and two-population settings is crucial.

The compartmentalization of one- and two-population models may, however, not always be appropriate. A two-population analysis requires that players exclusively receive their payoffs from interactions with the external population. Likewise, in a one-population setting, players never interact with opponents from other populations. Both these assumptions may not be warranted: why should players in a two-population game not interact at least occasionally within their own population? Why should agents in a single population setting not sometimes be also exposed to interactions with agents from other populations? It seems plausible that the interaction will often be mixed.

For non-human players, examples where the one- and the two-population cases overlap are abundant in resource conflicts. Animals will predominantly compete for resources with other members of the same species (intra-species competition). But there will also be inter-species competition (Birch, 1957)—think of different predatory mammals fighting for prey and water, or of various sessile organisms competing for light interception and soil. Inevitably, intra-specific and inter-specific competition overlap.[1]

An example with human players can be found in Mailath, (1998). Traders bargain either within their own village or encounter visitors from a different population. The game is hawk-dove in both cases but the analysis is one-population in the first

[1]Connell and Sousa, (1983) and Schoener, (1983) provide surveys of works on inter-specific competition. Kennedy and Strange, (1986) show how the density of salmon fry in an ecological niche appears to be influenced by the presence of both older salmons (same species, different generation) and trout (different species).

case and two-population in the second and the evolutionary selection mechanisms differ starkly. But beyond these polar cases traders may, of course, interact at the same time both with players from their own village and with visitors.[2]

The notion that intragroup and intergroup interactions overlap makes sense when agents do not condition their strategy on the population from which an opponent stems. This will be the case when players cannot identify which population a rival is from, that is, when group membership is determined by indiscernible factors such as geographic location and religious or political views. Even when they can identify the groups to which other players belong, they may still not be able or willing to condition their strategy on this identification.[3] A firm's strategy may involve a managerial structure or incentive scheme that cannot be switched on and off depending on whether the firm is interacting with its peers in a supply chain or with its customers or suppliers. Boundedly rational players may choose the same action for intragroup and intergroup interactions due to limited learning in complex environments. But rational agents may do the same in order to establish a global reputation, or as a result of the costly cognitive resources they employ to organize their reasoning (see section 1.2).

In this chapter, we analyze the interaction of one- and two-population dynamics, theoretically and in experiments. We analyze a uniparametric family that combines the two models by interpolating between both extremes with a coupling parameter κ which measures the weight of the intergroup interaction.[4] One- and two-population matchings are obtained for $\kappa = 0$ and $\kappa = 1$, respectively. We analyze the replicator dynamics of this system theoretically[5] and conduct the experiment in continuous time (Pettit et al., 2014). This is more suitable than standard discrete-time experiments for testing the predictions of evolutionary game theory, foremost because it allows for asynchronous choices and faster convergence.

[2]Somewhat similarly, Roll, (1994) interprets stock market traders performing fundamental analysis as doves and traders gathering information only from price movements as hawks. As suggested by a referee, Roll's original model is formulated for one population but could easily be extended to consider two populations, perhaps in different countries or different types of market participants, for example, pension funds vs. hedge funds.

[3]Taking a different approach, Selten, (1980) assumes that players can condition their strategy based on the information available to them.

[4]Independently, a similar approach has been developed by Friedman and Sinervo, (2016, section 3.7). Their starting point is a two-population model, and they introduce coupling in the form of "own-population effects." See also a previous analysis of evolutionary models with two groups of individuals in Cressman, (1995).

[5]Gómez-Gardeñes et al., (2012) use a similar model to analyze simulations of games on overlapping graphs.

Our application is a hawk-dove game. The hawk-dove game is the paradigm for the analysis of conflicts over scarce resources (Maynard Smith, 1982). Introduced by Maynard Smith and Price, (1973) in the context of animal conflict, it also became highly influential for human interactions due to its fairly simple definition which nevertheless generates very rich dynamics as a population game.

Oprea et al., (2011) analyze the hawk-dove game for the sign-preserving dynamics of the one- and the two-population case. Their (continuous-time) experiment confirms the predictions in that the symmetric mixed equilibrium is more likely to be selected in the one-population treatment whereas separation is stronger in the two-population treatment.

Our theoretical analysis confirms the existence of a bifurcation in the dynamics of the system, and the replicator dynamics predicts three regions with different stable equilibria. First, for any $\kappa < \kappa_m^*$ the predictions for the aggregate population strategy is a non-degenerate mixed equilibrium, as in the one-population setting ($\kappa = 0$). For $\kappa > \kappa_p^*$ pure play emerges for both groups, as in the two-population analysis ($\kappa = 1$). For the intermediate values $\kappa \in (\kappa_m^*, \kappa_p^*)$, a qualitatively novel prediction emerges where one population coordinates on a pure strategy while the second population is composed of a mixture of hawks and doves. This hybrid case does not occur with a single population or with two populations.

One way of interpreting these theoretical results is that the existing analyses of undiluted one- and two-population cases are robust with respect to perturbations. We find $\kappa_m^* = 1/2$ and show that κ_p^* will vary between a half and one. In words, the prediction of the one-population case extends with much overlap to a second population. A more moderate statement can be made regarding the two-population case as the scope for pure equilibria is typically smaller than the scope for mixed equilibria. In that sense, the two-population analysis seems somewhat less robust. Nevertheless, theoretically, it appears that neither of the one- nor the two-population cases are strongly affected by perturbations.

Our experimental results qualitatively confirm the predictions, but there are also departures from the theory. We find that mixed behavior is observed throughout where predicted—including the pure one-population treatment and the coupled variants with $\kappa < 1/2$. We also see a sound separation of hawks and doves in our pure two-population ($\kappa = 1$) treatment. These findings confirm and extend

the experiments of Oprea et al., (2011). Among the discrepancies between the replicator dynamics prediction and the experimental results is a general bias in the mixed strategies: in the treatments where the mixed equilibrium was expected, the frequency of hawk play was lower than predicted. As for the $\kappa \in (\kappa_p^*, 1)$ case (where a pure equilibrium is predicted), the separating effect is less pronounced than with $\kappa = 1$. The data further indicate that the splitting point (understood as the level of κ for which the populations split into two groups of "mostly hawks" and "mostly doves") experiences notable variations across sessions.

1.2 Literature

The implementation of interactions as population games recovers the spirit of the "mass action" interpretation of the mixed Nash equilibrium (Björnerstedt and Weibull, 1996; Young, 2011). Each player in a population can simply play a pure strategy, but the frequencies of the strategies in the population may correspond to a mixed Nash equilibrium. This relaxes the reasoning skills required for mixed play.

When the (static) game exhibits multiple equilibria, the evolutionary approach provides a powerful tool for equilibrium selection and learning (Friedman, 1996).[6] In a seminal contribution to evolutionary game theory, Friedman, (1991) compares the theoretical conditions for static stability in evolutionary games involving one and two (or more) groups of individuals, with applications to, for example, male-female mating problems. Weibull, (1995) attributes the first multi-population replicator dynamics analyses to Taylor and Jonker, (1978) and Maynard Smith, (1982).[7] Weibull, (1995) considers a different version of replicator dynamics for the n-population case. Following Nowak and May, (1992), a number of papers have also analyzed how the structure of a population may affect its behavior (Lieberman et al., 2005; Taylor et al., 2004).

Our starting point is that players choose the same action when playing the same game in encounters with players from different populations. This is in line with

[6] On learning issues, see Camerer and Ho, (1999), Hopkins, (2002), and Huck et al., (1999).

[7] Page and Nowak, (2002) explain different approaches to deterministic dynamics in population games. Hofbauer and Sandholm, (2002) show the connection between stochastic choice-making and deterministic dynamics. See Szabó and Fáth, (2007) or Sandholm, (2010) for comprehensive surveys.

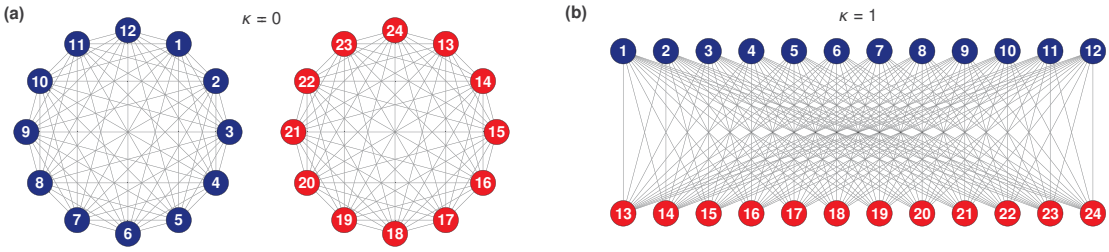

FIGURE 1.1: POPULATION STRUCTURES. *Network representation of (a) one-population and (b) two-population protocols with* 24 *players.*

Samuelson, (2001) who argues that agents facing a problem of multiple strategic interactions may balance the gains from better decision-making against the cost of using scarce cognitive resources. This can result in the application of the same choice in several of the interactions. Jehiel, (2005) formalizes the notion of "analogy-based expectation equilibrium" where players best respond to beliefs that are correct, on average, over various analogous situations. Huck et al., (2011) provide experimental evidence. Grimm and Mengel, (2014) analyze learning across games in experiments with the concepts of "belief bundling" and "action bundling" – both of which can imply that players simplify their decision environment by choosing the same action in different games, as a form of "best response bundling." See also Mengel, (2012) and the discussion contained therein.

1.3 Theory

We analyze the replicator dynamics with an even number of players divided into two (coupled) populations of equal size, labeled X and Y. We define the simplex $S^X = \{s^X = (s_1^X, s_2^X) : \sum_{a=1,2} s_a^X = 1\}$ such that any point in it represents the fraction of population X employing each available strategy.[8] S^Y is defined analogously for population Y. The product $\Omega = S^X \times S^Y$ is the set of strategy profiles and also the state space of the dynamical system. We focus on symmetric two-strategy games defined by 2×2 payoff matrices, with action set $S = \{s_1, s_2\}$. The matrix element π_{ij} defines the payoff from choosing action s_i when playing against pure strategy s_j. To simplify notation, let x and y be the share of the strategy s_1 in populations X and Y, respectively. The state vector of population X is $\omega_x = (x, 1-x)^T$, and $\omega_y = (y, 1-y)^T$ for population Y. Then, the dimensionality of

[8]Players could also be using a mixed strategy. This would not alter the analysis.

the problem is reduced to two, x and y, because the state of the dynamical system is a composite in the form $\omega = (x, 1-x; y, 1-y)^T \in \Omega$. Let $\mathcal{L}_\Pi : [0,1] \times [0,1] \to \mathbb{R}$ be a linear operator for any given 2×2 payoff matrix Π. Its application over a bidimensional vector w is defined as $\mathcal{L}_\Pi[w] = \langle e, \Pi w \rangle$, where we define $e = (1, -1)^T$ and $\langle \cdot, \cdot \rangle$ is the inner product in the vector space.

Consider the two standard matching protocols: the one-population protocol and the two-population protocol. In the one-population case, players interact randomly with other players from their population and so, technically, every player in a population earns the payoff of her choice against the aggregate strategy of her own population. With the two-population protocol, the row players (population X) play against the column players (population Y). See Figure 1.1 for a graphical representation of these population structures. In the one-population case for, say, population X, we can write the rate of growth of the strategy s_1 in the population as $\dot{x} = x(1-x)\mathcal{L}_{\Pi_A}[\omega_x]$. For population X in the two-population case, we write $\dot{x} = x(1-x)\mathcal{L}_{\Pi_B}[\omega_y]$. In general, we can consider different payoff matrices for the within-group and the between-groups games, Π_A and Π_B, respectively.

As our key novelty, we introduce a new matching protocol involving the coupling parameter $\kappa \in [0,1]$ which integrates the two protocols in a linear fashion. This coefficient is restricted to the unit interval, and its extremes $\kappa = 0$ and $\kappa = 1$ correspond to the one-population and the two-population settings, respectively. We then define the linear combination $\dot{x} = x(1-x)\big[(1-\kappa)\mathcal{L}_{\Pi_A}[\omega_x] + \kappa\mathcal{L}_{\Pi_B}[\omega_y]\big]$ generalizing the study to situations with a simultaneous existence of strategic interactions at both intra- and intergroup levels. The (instantaneous) payoff function for a player belonging to population X and choosing strategy $s_i \in S$ is given as

$$\pi_X(s_i; x, y)(t) = (1-\kappa)\big[\pi^A_{i1}x(t) + \pi^A_{i2}\big(1 - x(t)\big)\big] + \kappa\big[\pi^B_{i1}y(t) + \pi^B_{i2}\big(1 - y(t)\big)\big]. \quad (1.1)$$

Due to symmetry, π_Y is analogous and just requires the exchange of the population labels x and y.

We now simplify $\Pi_A = \Pi_B$ and choose the hawk-dove game for our analysis of intra- and intergroup interaction. The hawk-dove game can be parametrized as

$$\Pi_A = \Pi_B = \begin{pmatrix} a + \frac{1}{2}(v-c) & a+v \\ a & a + \frac{1}{2}v \end{pmatrix}, \quad (1.2)$$

where the parameters $0 < v < c$ represent the valuation of the good and the cost of the conflict, respectively, and $a > 0$ is the players' endowment.

We obtain the dynamics of the model as a system of coupled ordinary differential equations:

$$\begin{cases} \dot{x} &= x(1-x)\frac{1}{2}\big[v - c\big(x + \kappa(y-x)\big)\big] \\ \dot{y} &= y(1-y)\frac{1}{2}\big[v - c\big(y + \kappa(x-y)\big)\big]. \end{cases} \tag{1.3}$$

The rate of growth of each strategy in the population is determined solely as a function of: (i) the current state of the system (x, y), (ii) the value of the good v and the cost of the conflict c, and (iii) the coupling parameter κ.

This parameter κ represents the strength of the coupling between the two populations of players, while $(1-\kappa)$ is the weight of the interaction within each group. Depending on the context of application of the model, this can mirror different effects. For the traders in the example in Mailath, (1998), κ measures the fraction of players at the trade fair coming from a neighboring city. For the notion of best-response bundling in the experiments of Grimm and Mengel, (2014), our model can be seen as the mean field abstraction of a treatment where κ tunes the frequency in which each matching protocol appears.[9]

The following proposition formalizes the analysis of the dynamical system (1.3) and relates it to our notion of intra- and intergroup conflict. A proof can be found in the Appendix.

Proposition 1.1. *Given the replicator dynamics in (1.3):*

(a) if $\kappa < \kappa_m^*$, the mixed Nash equilibrium is selected,

(b) if $\kappa > \kappa_p^*$, the pure Nash equilibria are selected,

(c) in the intermediate range $\kappa_m^* \leq \kappa \leq \kappa_p^*$, a hybrid equilibrium is selected where one population plays a pure strategy and the other one chooses a mixture.

The cutoff points satisfy $\kappa_m^* = 1/2 \leq \kappa_p^*$ and $\kappa_p^* = \max\{v/c, 1 - v/c\}$. If $c = 2v$ then $\kappa_p^* = \kappa_m^* = 1/2$ and case (c) is void.

Proposition 1.1 contains the one-population and two-population cases from previous research (Oprea et al., 2011) as limit cases. The prediction for region (a) is as in the one-population matching ($\kappa = 0$) and the one for region (b) is as in the

[9]The definition can include asymmetric coupling with groups of different sizes or in situations where the populations weight the two conflicts in a different way, suitable in the meaning of animal competition.

Table 1.1: Fixed points' location. Replicator dynamics (1.3) with $v = 12$ and $c = 18$. See the appendix for the general solution.

Pure states	Hybrid states	Mixed states
$p_1^* = (0,0)$	$p_5^* = (0, 2/[3(1-\kappa)])$	$p_9^* = (2/3, 2/3)$
$p_2^* = (1,0)$	$p_6^* = (1, (2-3\kappa)/[3(1-\kappa)])$	
$p_3^* = (0,1)$	$p_7^* = (2/[3(1-\kappa)], 0)$	
$p_4^* = (1,1)$	$p_8^* = ((2-3\kappa)/[3(1-\kappa)], 1)$	

two-population matching ($\kappa = 1$). The hybrid equilibrium in region (c) is novel and exists neither as a Nash equilibrium nor as an attractor of the one-population or two-population settings. Table 1.1 gives the coordinates of the fixed points with parameters corresponding to the games played in the experiment (section 1.4).

In Figure 1.2, we illustrate the equilibrium selection for the parameters used in the experiment. For values of $\kappa < \kappa_m^* = 1/2$ the only attractor in the phase space corresponds to both populations being composed of two-thirds hawk. For $\kappa > \kappa_p^* = 2/3$, one group plays purely hawk and other one plays purely dove. For the intermediate range $\kappa \in [1/2, 2/3]$, the replicator dynamics predict a pure-mixed configuration such that the more hawkish population plays purely hawk ($x = 1$) while the more dovish group plays a completely mixed strategy.

Figure 1.2 (a) also shows the impact of the coupling on the phase portrait of the dynamical system. Starting with $\kappa = 0$, an increase in κ rotates the nullclines (zero-growth isoclines) $\dot{x} = 0$ and $\dot{y} = 0$ clockwise and counterclockwise, respectively. No qualitative change happens at the beginning, but between $\kappa = 0.2$ and 0.4 these nullclines cross the upper-left and bottom-right corner of the phase space and eliminate two saddle points. This does not have a major impact on the qualitative predictions. We obtain the first bifurcation in the system for $\kappa = 1/2$: both nullclines coincide and their intersection transforms from attractor to saddle point. Simultaneously, the remaining saddle points located at the edges become the attractors of the system. These attractors move along the edges when κ continues increasing. Finally, the second bifurcation occurs when they meet the two corner points $(1,0)$ and $(0,1)$ which become the attractors of the system.

Proposition 1.1 generates testable hypotheses. In addition to relying on the equilibrium predictions (mixed for $\kappa < 1/2$, pure for $\kappa > 2/3$), we will use a "separation index," $\Delta s(\kappa) \in [0,1]$. This index is defined as $\Delta s(\kappa) = \bar{s_1}(\kappa, X) - \bar{s_1}(\kappa, Y)$.

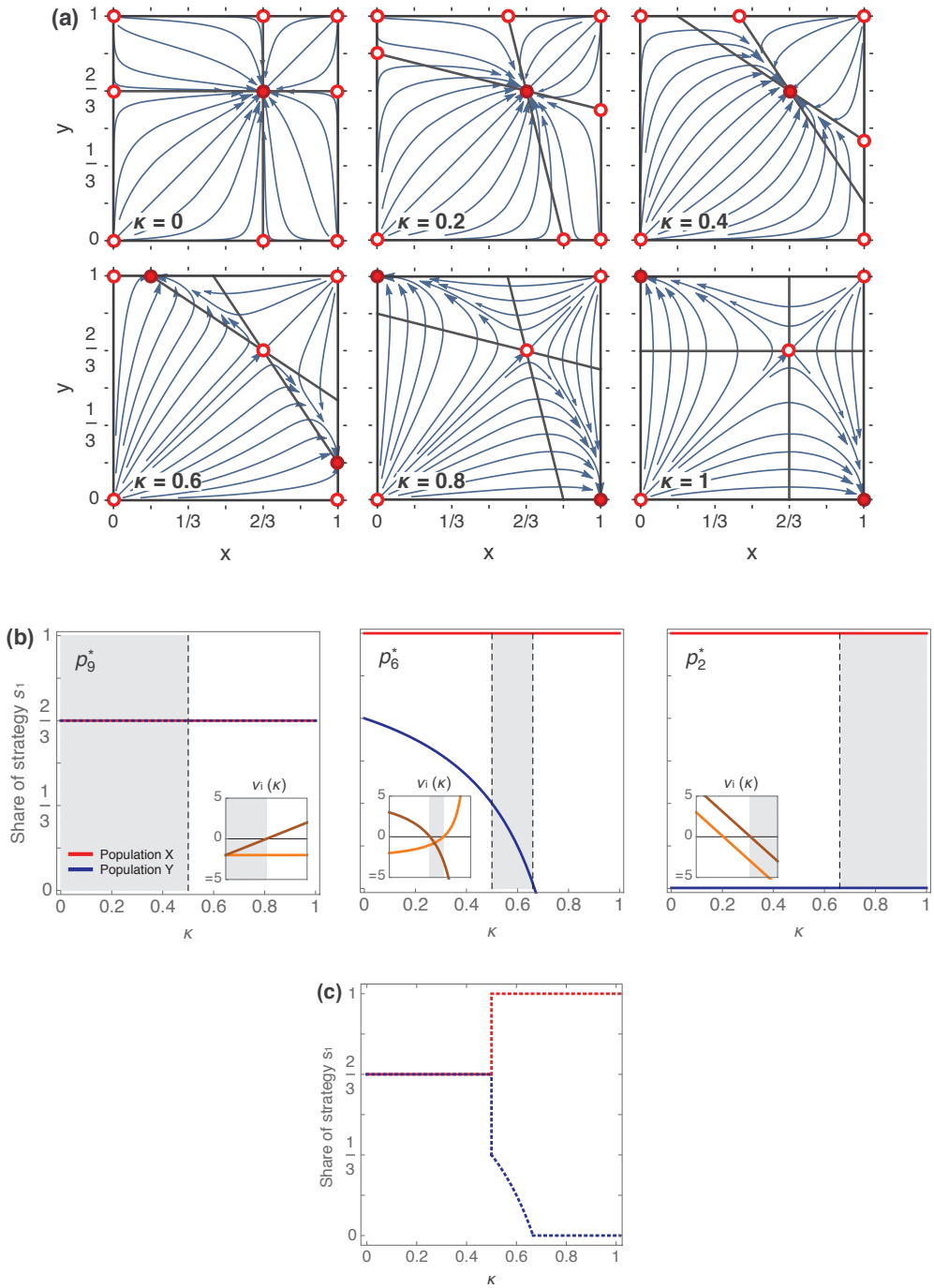

FIGURE 1.2: REPLICATOR DYNAMICS. Plots with $v = 12$ and $c = 18$. (a) Phase portrait of (1.3). White-filled points: non-stable. Red-filled points: stable. Dark lines: nullclines. (b) Share of strategy s_1 (hawk) in populations depending on κ. Shaded areas: stability domains (eigenvalues $\nu_i(\kappa)$ as inset and in this chapter's appendix). (c) Resulting bifurcation diagram.

That is, $\Delta s(\kappa)$ is the share of the hawk strategy in the more hawkish population minus the share of the hawk strategy in the more dovish population,[10] for a given value of the treatment variable κ. Using $\Delta s(\kappa)$ and interpreting Proposition 1.1 in a qualitative fashion, we obtain our main hypotheses:

$$\Delta s(0) = \Delta s(0.2) = \Delta s(0.4) < \Delta s(0.6) < \Delta s(0.8) = \Delta s(1). \tag{1.4}$$

1.4 Experiment

For the experiment, we choose the payoff parameters $a = 3$, $v = 12$, and $c = 18$. This results in the following hawk-dove game:

$$\Pi = \begin{pmatrix} 0 & 15 \\ 3 & 9 \end{pmatrix}. \tag{1.5}$$

The standard two-player game has three Nash equilibria of the form $(\sigma_X, \sigma_Y) \in \{(1,0),(0,1),(2/3,2/3)\}$, where σ_l denotes the probability that strategy hawk will be chosen by player $l \in \{X, Y\}$.

Our treatment variable is the coupling parameter κ. We consider $\kappa \in \{0, 0.2, 0.4, 0.6, 0.8, 1\}$. The cases $\kappa \in \{0, 0.2, 0.4\}$ correspond to Proposition 1.1 (a), the cases $\kappa \in \{0.8, 1\}$ to Part (b), and $\kappa = 0.6$ corresponds to Proposition 1.1 (c).

We use a within-subjects design and all subjects play all six treatments consecutively. To mitigate order effects or hysteresis, we randomize the order of the treatments at the session level (see Table 1.2). To prevent reputation effects and to maintain the one-shot character of the experiment, we employ random matching such that the composition of the groups changes at the beginning of each treatment. Players are independently and randomly assigned their initial actions in each treatment. Furthermore, subjects are paid only for one randomly-selected treatment in order to avoid wealth effects or hedging behavior across treatments (Blanco et al., 2010). This randomization is implemented with a public dice roll at the end of each session.

Other experimental procedures were as follows. All participants received hard-copies of the instructions at the beginning of the session, and afterwards these

[10] The label "population X" is arbitrarily assigned to the more hawkish group in the steady state for the analysis of the experimental data in the rest of the chapter.

Table 1.2: Sequence of treatments in each session

Period	Session 1	Session 2	Session 3	Session 4	Session 5	Session 6
1	$\kappa = 0.8$	$\kappa = 0.2$	$\kappa = 1$	$\kappa = 0.8$	$\kappa = 0.4$	$\kappa = 1$
2	$\kappa = 0.2$	$\kappa = 1$	$\kappa = 0.4$	$\kappa = 0$	$\kappa = 0.8$	$\kappa = 0.6$
3	$\kappa = 0$	$\kappa = 0.6$	$\kappa = 0.6$	$\kappa = 0.4$	$\kappa = 0.2$	$\kappa = 0.2$
4	$\kappa = 0.6$	$\kappa = 0$	$\kappa = 0$	$\kappa = 0.6$	$\kappa = 1$	$\kappa = 0.4$
5	$\kappa = 0.4$	$\kappa = 0.8$	$\kappa = 0.2$	$\kappa = 1$	$\kappa = 0$	$\kappa = 0.8$
6	$\kappa = 1$	$\kappa = 0.4$	$\kappa = 0.8$	$\kappa = 0.2$	$\kappa = 0.6$	$\kappa = 0$

were verbally summarized (see the instructions, available as online appendix). Each session began with a trial part consisting of three 90-second periods in which the players had the opportunity to familiarize themselves with the software. The subjects were aware that no payoffs would result from playing these three periods and we chose payoff matrices different from the hawk-dove games that would be used in the actual treatments. The six periods in which we ran the treatments had a time length of 210 seconds each. Subjects reported a good comprehension of the task and software in an anonymous questionnaire which they filled in at the end of the sessions.

The experiment was conducted with the software ConG. This software package has been made available in open-access by Pettit et al., (2014) and allows for experiments to be played in (virtually) continuous time.[11] This particular setting allows the players to make their choices in a fully asynchronous manner and they experience the updating of the system in real time. This framework is particularly suitable in our case because standard evolutionary models assume asynchronous updating by the agents and make long-run predictions which may be distorted if the experiments are performed as a finite sequence of synchronous repetitions of a stage game. See Oprea et al., (2011) on this issue.

Figure 1.3 shows two examples of the graphical display presented to the subjects in our experiment. On the left side of the screen, players could see the payoff matrices and the selection tool. Every agent was framed as a row player who needed to choose either A (hawk) or B (dove). The selection could be made with the radio buttons or with the up and down arrow keys. Subjects could change their action at any point in time and their choices had an immediate impact on

[11] We extended the basic package of ConG with a new payoff function, a customized matching scheme, and a new graphical interface adapted to the information set that needs to be displayed according to our design.

both games. The instantaneous choice was highlighted with a blue shadow in the selected row.

Players saw two payoff matrices: the left one refers to the interaction with the "own group" and the second one refers to the interaction with the "other group." The entries of these two matrices displayed are determined as $(1-\kappa)\Pi$ and $\kappa\Pi$, respectively, with Π defined in (1.5) and κ being the treatment variable (not known by players). Subjects were informed that the level of their payoff flow was determined as the sum of what they were simultaneously earning in the interactions with the own and with the other group. The upper-left corner indicates the accumulated payoff during the period and the remaining time.

The right half of the screen provides the players with all relevant information on the state of play. The top chart plots the average strategy (that is, the share of subjects choosing hawk) of each population. The middle chart documents the player's own choice, which can only alternate between A (hawk) and B (dove). The bottom chart plots a dark red solid line representing the payoff flow that the player is earning at a given point in time. The red shadow helps participants to understand that the payoff they earn is accumulated over time. The three charts share the same horizontal axis, that is, time. Note that all the changes of any factor are shown in the corresponding charts without any noticeable delay.

We ran six experimental sessions at the DICELab for experimental economics in Düsseldorf in April and May 2015. Each session comprised 24 subjects (two populations of 12 subjects each) with 144 subjects in total. Generally, participants were recruited from the local subject pool which contains students of various fields at the Heinrich Heine University of Düsseldorf, using ORSEE (Greiner, 2015).

1.5 Results

Figure 1.4 presents the data from all sessions and from all treatments. The vertical axis represents the share of players who chose hawk in the two populations of each session, at each instant. The horizontal axis represents time in seconds. This figure shows the evolution of the average strategy of the populations over time.

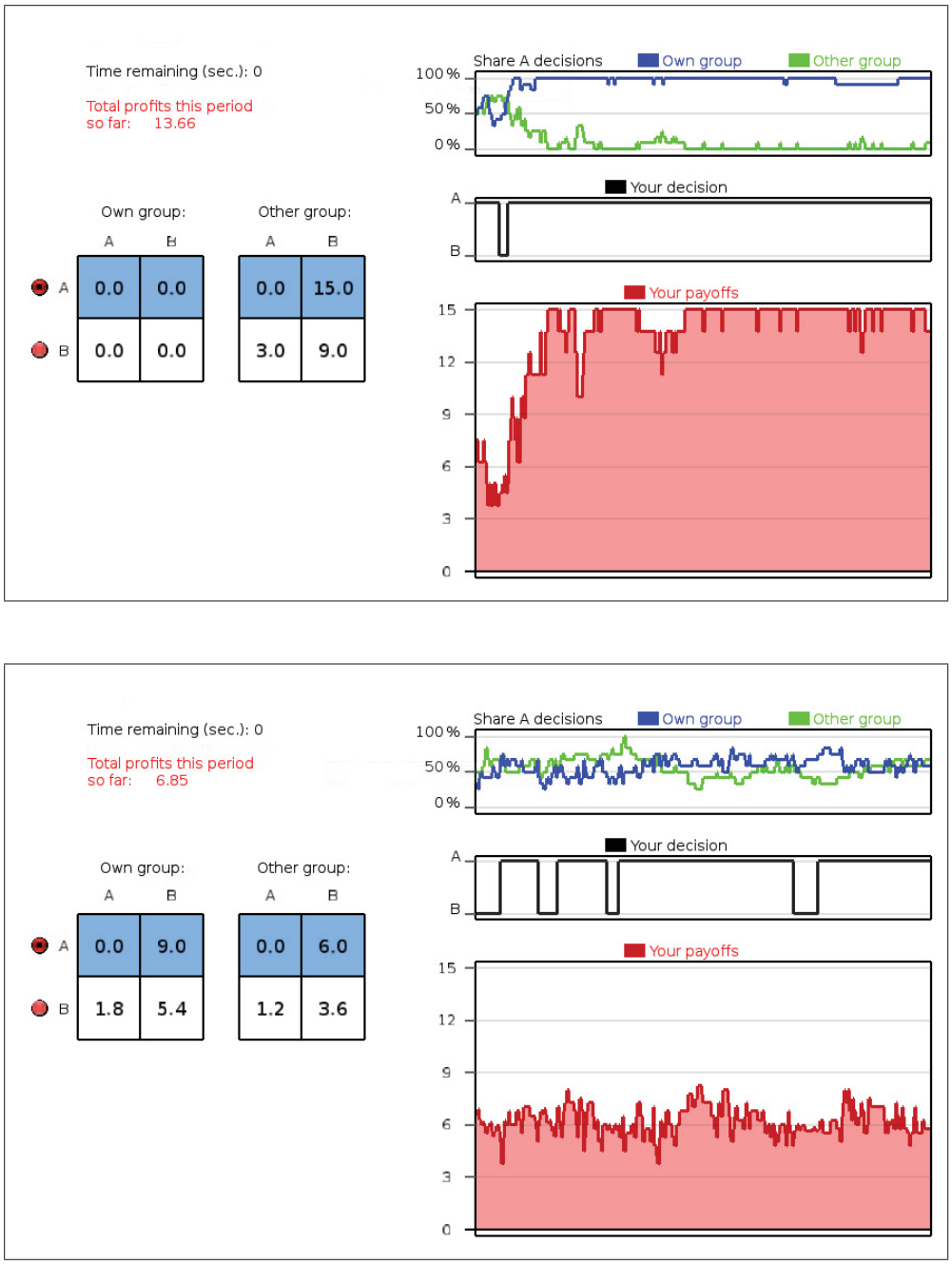

FIGURE 1.3: EXPERIMENTAL DISPLAY. Screenshot (translated from German) of two terminals at the end of two treatments. Top: player in a hawkish group in $\kappa = 1$. Bottom: player in a mixed-strategy group when $\kappa = 0.4$.

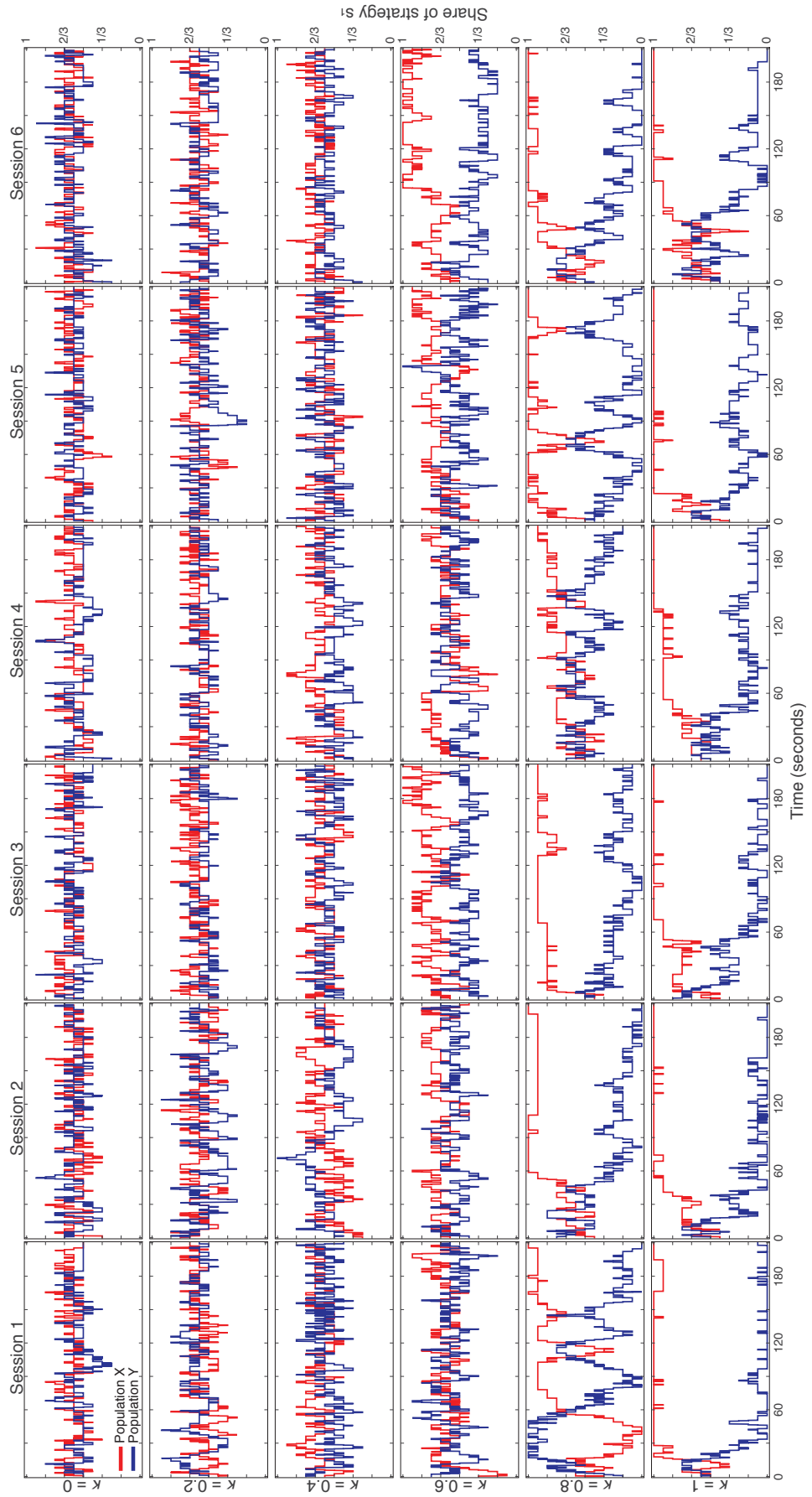

FIGURE 1.4: EXPERIMENTAL TIMELINES.
Evolution over time of the aggregate strategy of both populations, by treatment κ and session.

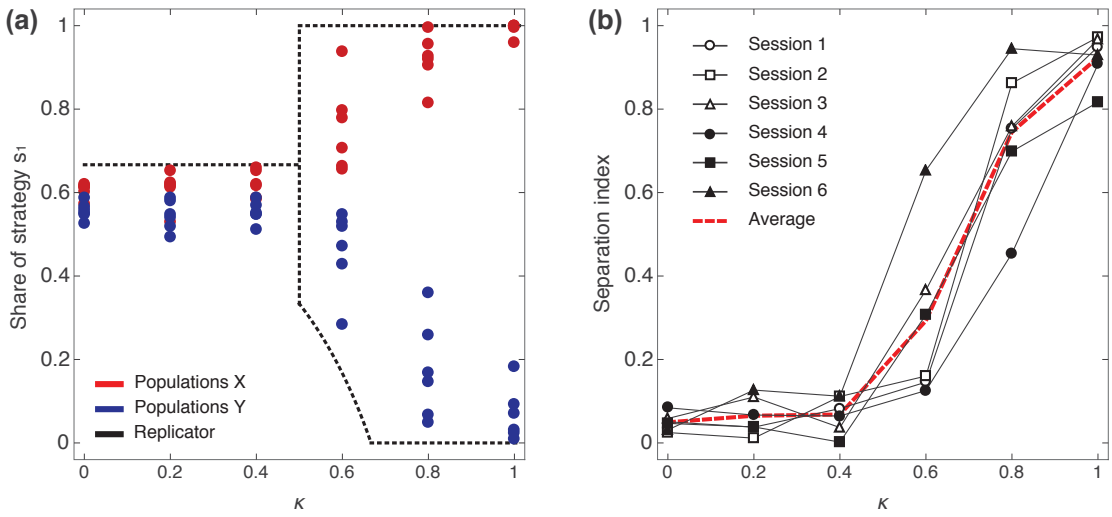

FIGURE 1.5: AGGREGATE RESULTS. (a) Share of hawk choices in steady state by κ in all sessions, compared to the bifurcation diagram in Figure 1.2. (b) $\Delta s(\kappa)$ for each session.

Consider first $\kappa \in \{0, 0.2, 0.4\}$ where both populations are expected to converge to the mixed equilibrium. Observed group behavior is in line with the predictions of two-thirds hawk, as can be seen in the first three rows of the plot. Also, the average strategies oscillate around that value in all 18 charts. When we consider the last 60 seconds of play as the steady state of the system, we find that the separation index $\Delta s(\kappa)$ is between 0 and 0.13 in all six sessions of these three treatments.

For $\kappa = 0.6$, theory suggests the hybrid case where one population should choose purely hawk while in the other population one-sixth hawkish play should emerge. Figure 1.4 shows this kind of outcome for sessions 3, 5, and 6 where we observe $\Delta s = 0.37$, 0.31, and 0.65, respectively. In the other three sessions, the steady state is more in line with the mixed equilibrium and we observe separation indices in the vicinity of 0.15, resembling the data in the treatments with a lower κ. The level of κ for which the populations separate appears to vary from session to session.

With $\kappa \in \{0.8, 1\}$, the average strategies of the two populations are predicted to converge to pure play in the steady state. In Figure 1.4, the last two rows of the graph show much polarization between the two populations at the end of the treatments. The average separation in the two-population treatment ($\kappa = 1$) is 0.93 whereas we obtain $\Delta s(0.8)$ between 0.70 and 0.95, except in session 4. In that session, we observe a period of experimentation with mixing behavior, with a slow and delayed departure toward a pure equilibrium, such that $\Delta s(0.8) = 0.45$.

Figure 1.5 summarizes how the populations in all sessions behave in the steady state (last 60 seconds of play). Panel (a) compares the aggregate results of all sessions to the bifurcation predicted by the replicator dynamics. We arbitrarily assign the population label X to the more hawkish population in the steady state. We observe three main effects. First, for $\kappa \in \{0, 0.2, 0.4\}$, mixing behavior occurs, but with a general downward bias in the share of hawk choices in all populations. Second, the scatter plot for $\kappa = 0.6$ and 0.8 shows considerable dispersion, and even though the existence of the bifurcation is apparent, the intensity of polarizing behavior is clearly weaker than predicted by the replicator dynamics. Third, most of the deviation from perfect separation in the last two treatments ($\kappa \in \{0.8, 0.1\}$) is driven by the dovish populations. When $\kappa = 1$, the share of hawk in the steady state of the hawkish populations is larger than $x = 0.99$ in five cases and $x = 0.96$ in the sixth (Session 1). By contrast, the share of strategy hawk in the dovish populations is non-zero throughout and reaches values of almost 20% in several sessions. For $\kappa = 0.8$ both the hawkish and the dovish populations deviate from perfect separation, but a similar argument still applies.

The finding that pure-strategy behavior is more pronounced for the hawk populations can be explained as follows. The separation into hawk and dove populations induces substantial payoff inequalities. (See also the discussion in Oprea et al., 2011, section 4.) In the more dovish population, some individuals foresee that their group is doomed to earn the lowest payoff and thus deviate systematically from their best response. There are two pure equilibria, and such deviating behavior of doves can be seen as an attempt to break the coordination and push play toward the more profitable equilibrium. This kind of behavior is rather apparent for $\kappa = 0.8$ (see Figure 1.4). In some sessions, the identity of the more hawkish population changes several times.

Panel (b) of Figure 1.5 plots the separation indices for each treatment, classified by session. Despite the subtleties described above, the statistical analysis qualitatively confirms the hypotheses (1.4) of the replicator dynamics. Wilcoxon signed-rank tests yield the following results, where two-sided p values above the (in)equality signs indicate whether or not the according null hypothesis is rejected:

$$\Delta s(0) \overset{p>0.999}{=} \Delta s(0.2) \overset{p>0.999}{=} \Delta s(0.4) \overset{p=0.031}{<} \Delta s(0.6) \overset{p=0.031}{<} \Delta s(0.8) \overset{p=0.062}{<} \Delta s(1). \quad (1.6)$$

There are no significant differences between the consecutive separation indexes with $\kappa \in \{0, 0.2, 0.4\}$, consistent with our prediction. We also confirm (1.4) in that $\Delta s(0.4) < \Delta s(0.6)$ and $\Delta s(0.6) < \Delta s(0.8)$ are statistically significant. Finally, and in a deviation from the prediction, the separation index for $\kappa = 1$ is weakly significantly larger than for $\kappa = 0.8$.

1.6 Conclusion

Equilibrium selection and learning in populations are prime targets for evolutionary game theory. We analyze what happens when intra- and inter-group interactions overlap. We predict a dynamical bifurcation from symmetric mixed to asymmetric pure equilibria in the hawk-dove game which depends on the frequency of interaction in the own vs. another (second) population. The transition occurs at an intermediate range of the coupling parameter κ. In the transition range, one population coordinates on a pure strategy while the second population is composed of a mixture of hawks and doves.

We also analyze to what extent human behavior matches the bifurcation in continuous-time experiments, extending a previous study by Oprea et al., (2011). Our experimental results largely confirm the hypotheses. One implication of the results is that the predictions for one-population and two-population settings are robust with respect to the presence of overlapping inter- and intragroup interactions. Nevertheless, the transition regime experiences notable variation across experimental sessions.

This chapter demonstrates the usefulness of continuous-time experiments in the analysis of intra- and intergroup interactions. Observations of actual bifurcations, together with other recent developments in the field such as the analysis of limit-cycles in rock-paper-scissors games (Cason et al., 2014), show a much improved degree of resolution with which experiments can study evolutionary forces.

Appendix - Proof of Proposition 1

Location of fixed points. We obtain the zero-growth curves directly from (1.3). Because of the linearity of the fitness functions, all the nullclines are simple lines in the plane:

$$\begin{aligned} &\dot{x} = 0 \to x = 0 && \dot{y} = 0 \to y = 0 \\ &\dot{x} = 0 \to x = 1 && \dot{y} = 0 \to y = 1 \\ &\dot{x} = 0 \to x = \frac{v - \kappa c y}{(1-\kappa)c} && \dot{y} = 0 \to y = \frac{v - \kappa c x}{(1-\kappa)c}. \end{aligned} \tag{1.7}$$

Fixed points are located at the different intersections of a horizontal and a vertical nullcline. Obviously, the corners of the state space are fixed points and represent possible equilibria in which both populations play pure strategies,

$$p_1^* = (0,0),\ p_2^* = (1,0),\ p_3^* = (0,1),\ p_4^* = (1,1). \tag{1.8}$$

There are four other possible points where one population plays a pure strategy while the other is mixed,

$$\begin{aligned} p_5^* &= \big(0, v/[(1-\kappa)c]\big), \quad p_6^* = \big(1, [v-\kappa c]/[(1-\kappa)c]\big), \\ p_7^* &= \big(v/[(1-\kappa)c], 0\big), \quad p_8^* = \big([v-\kappa c]/[(1-\kappa)c], 1\big). \end{aligned} \tag{1.9}$$

Finally, we also obtain a possible configuration in which both populations mix strategies in a symmetric manner,

$$p_9^* = (v/c, v/c). \tag{1.10}$$

Point p_9^* is always inside the unit square because $0 < v < c$. Nevertheless, the fixed points p_5^* and p_7^* only exist for $\kappa \in [0, 1 - v/c]$ while p_6^* and p_8^* only exist for $\kappa \in [0, v/c]$.

Linear stability analysis. The Jacobian J with matrix elements $J_{mn} = \partial \dot{m}/\partial n$ is defined by

$$\begin{aligned} 2 \times J_{xx}(x,y) &= v - 2vx + c\big[3x^2(1-\kappa) - \kappa y - 2x(1-\kappa-\kappa y)\big] \\ 2 \times J_{xy}(x,y) &= \kappa c x(1-x), \end{aligned} \tag{1.11}$$

with J_{yx} and J_{yy} given by symmetry ($x \leftrightarrow y$). Stable points are those fixed points for which both eigenvalues of J (evaluated at the point's coordinates) are negative (Hofbauer and Sigmund, 2003). The eigenvalues are the two roots of the characteristic polynomial $\det\left[\nu\mathbb{I}_2 - J\right]$.

For p_1^* and p_4^*, we obtain $\nu_1 = \nu_2 = v/2 > 0$, and $\nu_1 = \nu_2 = (c - v)/2 > 0$, respectively. These two symmetric equilibria in pure strategies are never attractors of the system. For the asymmetric equilibria in pure strategies (p_2^*, p_3^*), the eigenvalues are $\nu_1 = (c - v - \kappa c)/2$, and $\nu_2 = (v - \kappa c)/2$. If $c < 2v$, then $\nu_2 > \nu_1$ and the asymmetric pure equilibria are stable for $\kappa \in [v/c, 1]$. If $c > 2v$, then $\nu_1 > \nu_2$ and they are stable for $\kappa \in [1 - v/c, 1]$.

Considering p_5^* and p_7^*, the eigenvalues are $\nu_1 = v - v/[2(1 - \kappa)]$, and $\nu_2 = [v^2 - (1 - \kappa)cv]/[2c(1 - \kappa)]$. Note that ν_1 is negative for $\kappa \in (1/2, 1)$, and ν_2 is negative for $\kappa < 1 - v/c$. These two points are stable for $\kappa \in [1/2, 1 - v/c]$, when $c > 2v$. For the points p_6^* and p_8^*, the eigenvalues are $\nu_1 = (c - v)(2\kappa - 1)/[2(\kappa - 1)]$, and $\nu_2 = (c - v)(\kappa c - v)/[2c(1 - \kappa)]$. ν_1 is negative for $\kappa \in (1/2, 1)$ and ν_2 is so for $\kappa < v/c$. Thus, these points are stable for the range $\kappa \in [1/2, v/c]$, provided $c < 2v$.

Finally, the symmetric equilibrium in mixed strategies p_9^* yields eigenvalues $\nu_1 = v(v - c)/2c$, and $\nu_2 = v(c - v)(2\kappa - 1)/2c$. The first one is constant and always negative since $c > v$ in the hawk-dove game. The second is negative for $\kappa < 1/2$, so p_9^* is stable when $\kappa \in [0, 1/2]$.

Thus, we have characterized the attractors of the dynamical system (1.3) to be selected for each region of the coupling parameter κ. These results are summarized in Proposition 1.1 and illustrated in Figure 1.2.

Declaration of contribution

Hereby I, Ismael Martínez Martínez, declare that this chapter, entitled "Equilibrium selection with coupled populations in hawk-dove games: Theory and experiment in continuous time" is co-authored with Volker Benndorf and Hans-Theo Normann.

I have contributed substantially to the conception of the project, the development of the model, the programming of the experimental software, the analysis and graphical representation of the results, as well as the writing of the final manuscript.

Signatures of the coauthors:

Volker Benndorf

Hans-Theo Normann

Chapter 2

Perturbed best response dynamics in a hawk-dove game☆

Summary of the chapter

We linearly interpolate between the evolutionary one- and two-population models of a hawk-dove game and examine the impact of behavioral noise on equilibrium selection. We find that perturbed best response dynamics generates two hypotheses in addition to the bifurcation predicted by standard replicator dynamics. First, when replicator dynamics suggests mixing behavior (close to the one-population model), there will be a bias against hawkish play. Second, the polarizing behavior that replicator dynamics predicts in the vicinity of the two-population model will be less extreme in the presence of behavioral noise. Both effects are clearly present in our experimental data set.

☆This chapter is co-authored with Volker Benndorf.

2.1 Introduction

Evolutionary and learning processes are key to understand the dynamics of equilibrium selection and to analyze departures from the best-response paradigm (Goeree and Holt, 1999; Mailath, 1993; Sandholm, 1998). Hofbauer and Sandholm, (2002) derive convergence results and show that asymptotic behavior is obtained in terms of the perturbed best response (PBR) dynamics. This family of models introduces random disturbances in the definition of the best response correspondences. The main result about deterministic representability of the stochastic process holds independent of the distributional assumptions about the random component. See Blume, (1993), Hofbauer and Hopkins, (2005), and Hopkins, (2002).

The logit choice function is a prominent model of PBR which is in line with standard random utility models. Players exhibit bounded rationality and behave as myopic best repliers who tremble in their decisions. They update their actions in a probabilistic manner such that better alternatives are chosen more frequently than others. This system can show configurations that replicator dynamics cannot explain. Traulsen et al., (2010) provide evidence supporting this model of strategy updating in human behavior. Alós-Ferrer and Netzer, (2010) and Zhuang et al., (2014) characterize long run properties of the logit response dynamics.

In this chapter, we focus on the application of logit response dynamics in a hawk-dove game, extending the analysis of a recent experiment by Benndorf et al., (2016) (Chapter 1). As a static interaction, this game exhibits a symmetric NE in mixed strategies and two polarized NE in pure strategies where one agent plays hawk and the other chooses dove. Basic intuition in population games is sufficient to argue that mixing behavior emerges when the game is played within the population (one-population matching) because only symmetric equilibria can survive (see Oprea et al., 2011). The polarized case is more likely to be observed in the between-populations matching (two-population model). The transition between both regimes of equilibrium selection has been observed in a novel experiment by linearly interpolating both extreme structures with a coupling parameter $\kappa \in [0, 1]$ (Benndorf et al., 2016, Section 5). The one-population case corresponds to $\kappa = 0$ and the two-population case to $\kappa = 1$.

As the benchmark case for comparison, replicator dynamics predicts symmetric mixed play with $\frac{2}{3}$ of hawk play for $\kappa < \frac{1}{2}$. A sudden bifurcation happens at $\kappa = \frac{1}{2}$

such that one population plays pure hawk and the other plays mixed strategy with $\frac{1}{3}$ of hawk. Separation increases monotonically on κ in the interval $[\frac{1}{2}, \frac{2}{3}]$ and the system is totally polarized for $\kappa > \frac{2}{3}$.

The PBR model applied to our experimental setting makes two strong predictions that go beyond the scope of the best-response paradigm of replicator dynamics. First, the share of hawk choices in the symmetric mixed equilibrium will be lower than $\frac{2}{3}$. Second, PBR implies that the impact of the polarizing forces on the behavior of the system will be weaker than suggested by replicator dynamics. This effect has two interpretations (see further explanation of the model below): the separation (difference in the share of hawk play) between the two populations will be lower than predicted by replicator dynamics. An alternative perspective is that the value of the coupling parameter κ for which the system transits from the mixed regime to the asymmetric configuration will be higher than $\frac{1}{2}$.

2.2 PBR model

We consider two populations of players (X and Y) in a two-strategy environment. Let $S^X = \{(s_1, s_2) : s_1^X + s_2^X = 1\}$ such that any point in it represents the share of each strategy among population X (equivalent definition for population Y). The pair (x, y) gives the state of the system, with $x = s_1^X$ and $y = s_1^Y$, respectively. Information about s_2 is redundant.

In order to capture the bifurcation, we interpolate the play of the game between the one- and the two-population models with a coupling parameter $\kappa \in [0, 1]$. If $\kappa = 0$, the player only participates in interactions within the population. If $\kappa = 1$, we recover the play between populations. Intermediate values of κ correspond to simultaneous interaction at the intra- and intergroup level (Benndorf et al., 2016, Section 3). The instantaneous payoff earned by a player in population X choosing strategy s_i for a given state of the system (x, y) is $\pi_X(s_i; x, y) = (1-\kappa)[\pi_{i1}x + \pi_{i2}(1-x)] + \kappa[\pi_{i1}y + \pi_{i2}(1-y)]$ where π_{ij} are the elements of a 2×2 payoff matrix.

According to the logit response function, a player in population X who observes a choice profile in the populations (x, y), and given the chance to revise the play,

chooses action s_1 with probability

$$p_X(s_1;\, x, y) = \frac{1}{1 + e^{-\lambda \Delta\pi_X(x,y)}}. \tag{2.1}$$

$\Delta\pi_X(x, y) = \pi_X(s_1;\, x, y) - \pi_X(s_2;\, x, y)$ is the payoff advantage (in population X) of strategy s_1 over strategy s_2. Analogous for Y. The comparison of profits influences the dynamics of the system weighted by $\lambda \in [0, \infty)$. This parameter captures deviations from the best response function. If $\lambda = 0$, the revision mechanism is independent from the payoff structure of the game and the system evolves toward an equal share of strategies in the populations. When $\lambda \to \infty$, PBR mirrors replicator dynamics.

We define the action set $S = \{s_1, s_2\}$ such that s_1 corresponds to strategy hawk, and s_2 to dove. Then, the hawk-dove game in matrix notation is

$$\Pi = \begin{pmatrix} a + \frac{1}{2}(v - c) & a + v \\ a & a + \frac{1}{2}v \end{pmatrix}. \tag{2.2}$$

This game represents a conflict of cost c over a scarce resource of value $0 < v < c$, and $a > 0$ is an endowment of the players. With these parameters (and the payoff function above) we obtain the fitness function $\Delta\pi_X(x, y) = \frac{1}{2}[v - c(x + \kappa(y - x))]$. $\Delta\pi_Y$ comes by symmetry.

The deterministic dynamics is defined by the system of coupled differential equations

$$\begin{cases} \dot{x} &= p_X(s_1;\, x, y) - x \\ \dot{y} &= p_Y(s_1;\, x, y) - y, \end{cases} \tag{2.3}$$

with p_X and p_Y defined in (3.14). A rest point of (2.3) corresponds to the logit quantal response equilibrium (McKelvey and Palfrey, 1995) for the given value of the parameter λ.

We illustrate the predictions of the PBR model in Figure 2.1. In panel (a), we see the stable manifold of the logit response dynamics in the hawk-dove game with the bifurcation as a function of the coupling parameter κ. As shown in panel (b), the prediction for $\lambda = 0$ is independent of the coupling condition and corresponds to uniform randomization. When λ increases, the system presents a bifurcation diagram that becomes closer to the prediction with replicator dynamics the higher the value of λ.

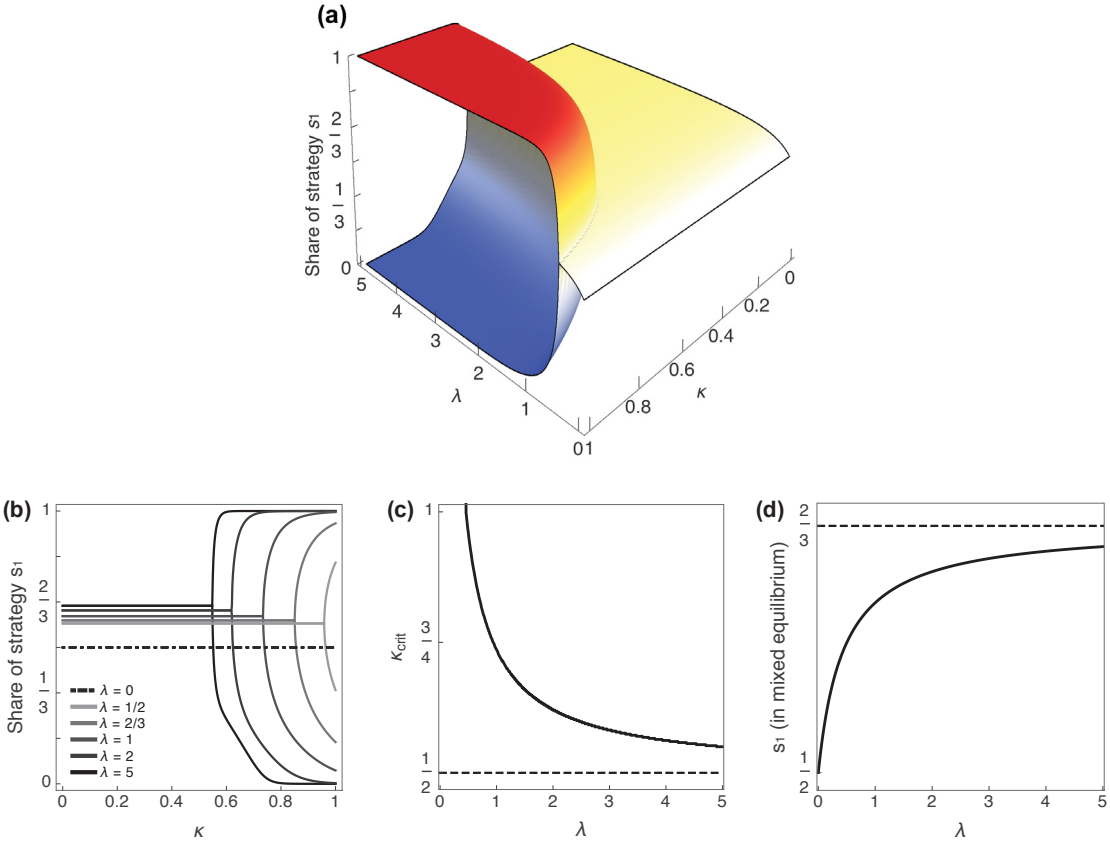

FIGURE 2.1: PBR PREDICTIONS. Parameters $a = 3$, $v = 12$ and $c = 18$. (a) Stable manifold. (b) Bifurcation diagrams. (c) Location of κ_{crit}. (d) Share of s_1 in mixed equilibrium, as functions of λ.

For every sufficiently high value of the rationality exponent λ (equivalent to very low levels of noise in the best response correspondences of the players), there exists a critical value κ_{crit} such that the equilibrium stability shifts from the mixed configuration toward a more polarized one. We compute κ_{crit} as a function of λ in panel (c). This value converges monotonically toward $\frac{1}{2}$ when the PBR model degenerates in the replicator dynamics ($\lambda \to \infty$). A similar logic applies to the share of the hawk choices in the populations for the regime with low coupling ($\kappa < \kappa_{\text{crit}}$). We illustrate in panel (d) how the level of hawk play monotonically increases with λ and converges to the mixed NE, $v/c = \frac{2}{3}$, when $\lambda \to \infty$.

From this discussion, we see that the PBR model generates two testable hypotheses about human behavior in the experiment:

H1. The share of hawk choices in the populations X and Y for treatments with $\kappa < \frac{1}{2}$ will be lower than $v/c = \frac{2}{3}$ and higher than $\frac{1}{2}$.

H2. The observed separation between populations (difference between hawk play in groups X and Y) for the treatment with $\kappa = 0.6$ will be lower than $\frac{5}{6}$.

Formulation of *H2* deserves some explanation. As discussed above, the presence of noise in the best response function shifts the location of the critical level of the population coupling κ_{crit} for which polarization begins (upward shift increasing in λ). It is not possible to make an ex-ante point prediction for λ and one cannot cover all possible values of κ as a treatment variable. Therefore, the exact point κ_{crit} cannot be directly observed in an experiment; however, we can identify the effect of the upward shift by measuring how buffered is the polarizing incentive perceived by the players with respect to the prediction with replicator dynamics. According to the PBR model, the higher the κ_{crit}, the smaller the separation reached by the populations for a fixed level of coupling, $\kappa = 0.6$. See Figure 2.1-Panel (b) and Figure 2.3.

2.3 Experiment

In this chapter, we utilize the dataset generated in an experiment by Benndorf et al., (2016). Subjects played the hawk-dove game with parameters $a = 3$, $v = 12$, and $c = 18$. The payoff entries are $\pi_{11} = 0$, $\pi_{12} = 15$, $\pi_{21} = 3$, and $\pi_{22} = 9$. The static game presents three NE as already mentioned. The two NE in pure strategies are equivalent and imply coordination of the two groups in opposite strategies, $(1, 0)$ or $(0, 1)$. The third equilibrium is symmetric in mixed strategies with a share $v/c = \frac{2}{3}$ of hawk choices in each population.

The coupling parameter κ was the treatment variable and took the six values from 0 to 1 with step $\Delta\kappa = 0.2$. Logit response dynamics predicts symmetric mixed play for the three treatments with lower κ. Separation can occur for the three other cases.

The experiment varied the treatments within subjects. All participants played all six treatments consecutively and the order of these treatments was randomized at the session level. The composition of the groups was randomized at the treatment level and players were independently and randomly assigned their initial actions

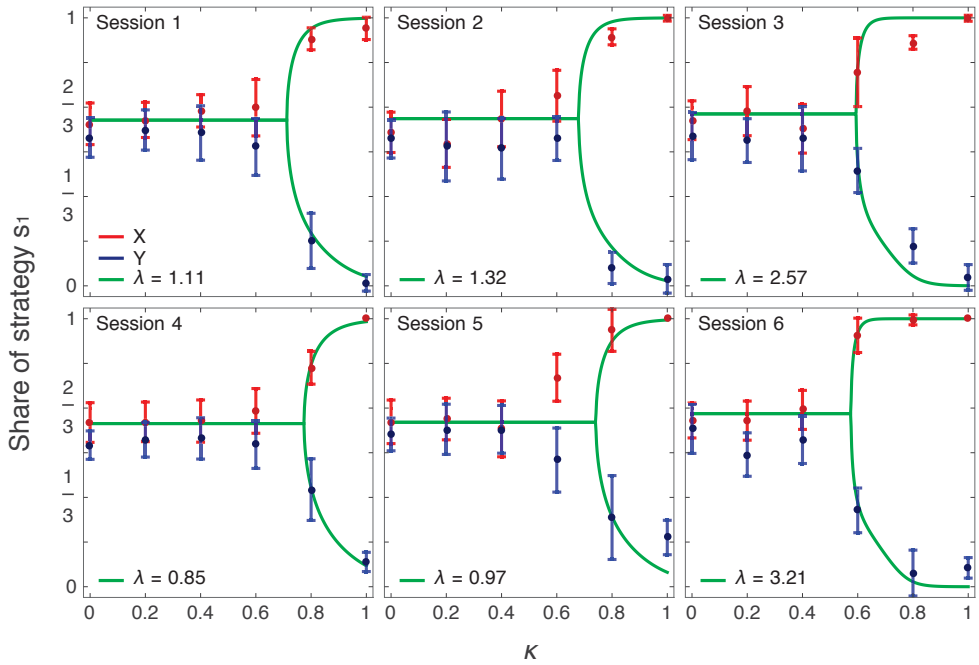

FIGURE 2.2: EXPERIMENTAL RESULTS (I).
Steady states for each κ and fit of PBR dynamics, by session.

in each treatment. Each treatment lasted 210 seconds of play. Only one treatment was paid, selected with a random draw at the end of the session. There were six experimental sessions and we employed a total of 144 participants. All sessions took place at the DICELab for experimental economics in Düsseldorf, in Spring 2015.

The experiment was conducted in (virtually) continuous time with ConG (Pettit et al., 2014). This environment is relevant to experiments in evolutionary dynamics because it allows for asynchronous choice making by the players and implements real time updating of the information set displayed to the agents.[1]

2.4 Results

Figure 2.2 reports the experimental results at the session level. We considered the last 60 seconds of play for the computation of the steady state of the system in each treatment (total length is 210 seconds). The two scatter plots (red and blue) show the share of strategy hawk in the two populations together with the error

[1]Further details about other procedures can be found in Benndorf et al., (2016, Section 4).

bar. Label X is arbitrarily assigned to the more 'hawkish' population in the steady state. As anecdotal information, we show a fit of the PBR model at the session level, with the estimated values of λ as inset.[2] For the sake of completeness, the best fit when considering a unique value of λ for the whole data set is for 2.51.

The two hypotheses stated by our PBR model can be tested directly from the experimental data set and are independent of any consideration about the fit of the parameter λ. In order to test the first hypothesis, we take the steady states reached during the three treatments with $\kappa = 0$, 0.2 and 0.4 in the six sessions. In total, we have 36 measurements of the share of hawk play in the range [0.493, 0.660]. However, our experimental design generates only one independent observation per session. Each session gives six data points: two populations, X and Y, times three treatments $\kappa \in \{0, 0.2, 0.4\}$. Thus, in order to perform the quantitative tests, we average the steady state of the two populations X and Y across the three mentioned treatments to get one observation per session. These six data points lie in the range [0.551, 0.597]. One-sided sign tests reject the null hypotheses that the median of the data points is less than or equal to $\frac{1}{2}$ and greater than or equal to $\frac{2}{3}$ with p-values of 0.0156 in both cases. The same test fails to reject the null hypotheses that the median of the data points is greater than or equal to $\frac{1}{2}$ and lower than or equal to $\frac{2}{3}$ with p-values of 1 in both cases. Hence, we can confirm the hypothesis *H1* of the PBR model in that the play of hawk strategy in the mixed regime belongs to the interval (1/2, 2/3). For our sample, average play of hawk is 0.583 with standard deviation of 0.017.

Regarding the second hypothesis, we have six measures of the separation between populations for the treatment with $\kappa = 0.6$. We define the separation index $\Delta s(\kappa) \in [0, 1]$ as $\bar{s}_1(\kappa, X) - \bar{s}_2(\kappa, Y)$. The separation index is the share of strategy hawk in the more hawkish population (X) minus the share of strategy hawk in the more dovish group (Y), for a given treatment κ. The observations span the range [0.126, 0.653], with average of 0.293 and standard deviation of 0.201. The one-sided sign test rejects the null hypothesis that the median of the data points is greater than or equal to $\frac{5}{6}$ (≈ 0.833) with a p-value of 0.0156 and cannot reject the null hypothesis that the median of the data points is lower than or equal to $\frac{5}{6}$ with

[2] Grid search on the values of λ with resolution $\Delta\lambda = 10^{-2}$ considering the distance $\sum_\kappa [x^*(\kappa) - \bar{s}_1^X(\kappa)]^2 + [y^*(\kappa) - \bar{s}_1^Y(\kappa)]^2$ as the objective function to minimize, where (x^*, y^*) is the PBR prediction (as a function of λ) and $\bar{s}_1$ is the observed share of hawk play in the steady state for the corresponding population and treatment.

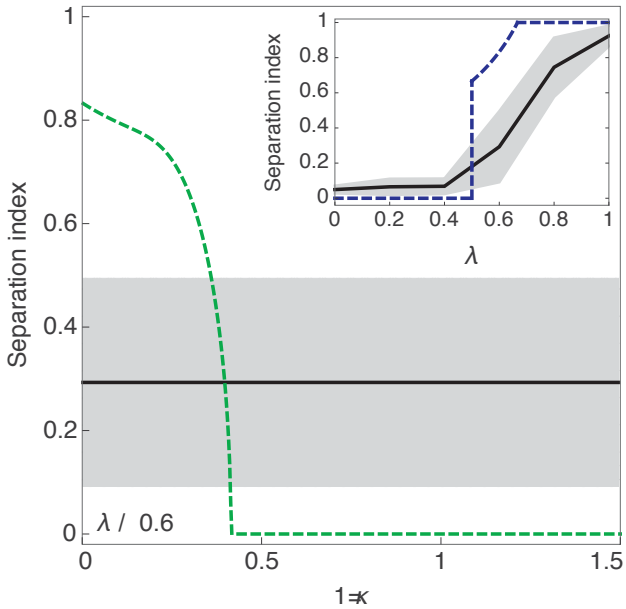

FIGURE 2.3: EXPERIMENTAL RESULTS (II). Separation index for $\kappa = 0.6$. PBR prediction as a function of λ (dashed green) and experimental observation (solid black). Inset shows the observed separation for all treatments (solid black) compared to the replicator prediction (dashed blue). Gray bands indicate standard deviations.

a p-value of 1. The data set confirms *H2* in that the observed separation between the populations for $\kappa = 0.6$ is clearly below the prediction under perfect rationality. Figure 2.3 compares the separation observed in the treatment with $\kappa = 0.6$ to the corresponding model predictions as a function of the level of noise (inverse of λ). The inset also shows the separation observed throughout all the treatments in comparison with the sharp step function predicted by replicator dynamics. The departure from the best-response paradigm in the way subjects played the games is clear, given our two experimental results being highly significant.

2.5 Discussion

In this chapter, we tested two deviations from replicator dynamics of qualitative nature. We characterized two traits of human behavior in a dynamic environment –the bifurcation of the hawk-dove game– that are predicted by PBR dynamics and that represent a systematic departure from the best response assumption that underlies the definition of replicator dynamics. Our results relate to other recent applications of PBR models, for example, to the experimental study of limit

cycles in rock-paper-scissors games by Cason et al., (2014); and to other recent characterizations of noise in behavioral dynamics in experimental games (Lim and Neary, 2016; Mäs and Nax, 2016).

To conclude, we acknowledge the ongoing debate concerning the informative value of estimating the parameter λ to compare point predictions between quantal response equilibrium and Nash equilibrium (see, for example, Brunner et al., (2011), Goeree et al., (2005), Haile et al., (2008), and Selten and Chmura, (2008) on this issue). We would like to emphasize that the two experimental results presented in this chapter are independent of any numerical fit of the parameter λ. The tests that we performed rely purely on the experimental observations; we offered estimates of λ in Figure 2.2 only for illustrative purposes.

Declaration of contribution

Hereby I, Ismael Martínez Martínez, declare that this chapter, entitled "Perturbed best response dynamics in a hawk-dove game" is co-authored with Volker Benndorf.

I have contributed substantially to the conception of the project, the development of the model, the analysis and graphical representation of the results, as well as the writing of the final manuscript.

Signature of the coauthor:

Volker Benndorf

Chapter 3

A general model for 2×2 games with coupled populations

Summary of the chapter

This chapter generalizes the linear model of replicator dynamics with coupled populations of Chapter 1 (Benndorf et al., 2016) to situations where the intra- and intergroup interactions can be any pair of 2×2 games, Π_A and Π_B. Using an angular representation of the games, only three parameters are relevant for equilibrium predictions: one angle defining each game, ϕ_A and ϕ_B; and the coupling parameter κ. In this model, κ arises naturally as the comparison between the scaling factors of the two payoff matrices. A comprehensive classification of this family of coupled interactions with replicator dynamics predicts a total of twenty-one qualitatively different scenarios of equilibrium predictions. Following the findings in Chapter 2, the analysis with perturbed best response dynamics weakens some of the evolutionary forces and reduces the number of qualitatively different scenarios to four. These results open the door for designing a future and exhaustive experiment.

3.1 Introduction

The majority of the literature on evolutionary game theory focuses on models where agents are grouped in one or two (sometimes more than two disjoint) populations, and where the interaction takes place either only within the own population or only with the other population. In both cases, the agent's payoff is determined by her own action that is confronted with the average strategy of the own population or the other population, respectively.

The notion that agents interact exclusively within their own population or exclusively with the other population is disputed, as already stated in Chapter 1. Benndorf et al., (2016) analyze the coupled model that linearly interpolates between both extreme population cases while keeping the same payoff matrix for both interactions. The question of why should players in a two-population setup not at least occasionally interact with players from their own population is also proposed in Friedman and Sinervo, (2016, Section 3.7) with the introduction of "own-population" effects that arise when players' actions in the two-population setup also have an impact on their peers in their own population.

Beyond the introduction of perturbations in the matching protocol for a given base game, coupled models also open the possibility to connect or overlap any two population games. Put differently, in a coupled model, intra- and intergroup interactions may differ qualitatively. As a consequence, coupled models allow for the analysis of a broad spectrum of intra- and intergroup interactions. The interaction with the own population might, for example, resemble a prisoners' dilemma while the interaction with the other group may have the characteristics of a hawk-dove game; this would be a typical situation where a group is subject to the free riding problem in the provision of public goods within the own population at the same time that they face a conflict over scarce resources with a competing neighboring population. One could also imagine a situation such that the two games present pure dominance but in opposite strategies: it is clear what to do within the own group and what to do against the other group, but both choices have conflicting motivations that cannot be disentangled.

Many combinations are possible and applicable to model different scenarios; therefore, this chapter takes an integrative approach. We perform an exhaustive analysis of equilibrium selection with coupled populations by modeling the dynamics of the

system with a minimal set of three parameters that nevertheless contains all the relevant information for equilibrium predictions and allows for any pair of 2×2 games to be represented. We find a total of twenty-one different analytical scenarios for replicator dynamics which we see reduced to four families of behavioral patterns with the introduction of noise in perturbed best response dynamics.

The model presented in this chapter extends and complements the one in Chapter 1 by taking a more general perspective in two directions. First, we consider the matrices Π_A and Π_B to be any pair of matrices in general, either the same or different, so the study presented here will contain the predictions stated in Benndorf et al., (2016) as possible subcases within a broader picture. The complexity in the analysis of the system is reduced by introducing an angular definition of the payoff matrices such that only two angular variables, $\phi_A, \phi_B \in [0, 2\pi)$, are required to specify the nature of the interactions and the conditions for equilibrium selection. Second, the parametrization of the model proposed in this chapter gives rise to the coupling parameter κ from very basic considerations; κ was introduced in Chapter 1 as an assumption in the definition of the linear coupling. In this sense, the linear interpolation used along this thesis in Chapters 1 and 2 is now derived naturally from the linearity induced by the usage of payoff matrices in the definition of the utility functions of the players. These results strengthen the validity of the experimental design employed in the first two chapters and propose a further research agenda.

3.2 Basic coupled model

We choose the family of symmetric two-strategy games that can be represented with 2×2 payoff matrices. We consider two games: a within-population game Π_A, and a game Π_B between the populations. These two coupled populations are labeled X and Y.

The action set is $S = \{s_1, s_2\}$. The simplex $S^X = \{s^X = (x, 1-x)\}$ with $x \in [0, 1]$ is such that any point s^X represents the fraction of agents of population X that are choosing each available strategy. S^Y goes by analogy; and x and y are the share of strategy s_1 in populations X and Y, respectively. Because of the normalization condition, the pair (x, y) is sufficient to know the state of the system.

We analyze the replicator dynamics where the players participate simultaneously in the two games Π_A and Π_B. The payoff entry π_{ij}^A (or π_{ij}^B) determines the payoff obtained in game A (or B) by a player who chooses action s_i and confronts pure strategy s_j. In the case of a player in population X the instantaneous payoff function is

$$\pi_X(s_i; x, y) = \pi_{i1}^A x + \pi_{i2}^A (1 - x) + \pi_{i1}^B y + \pi_{i2}^B (1 - y). \tag{3.1}$$

Compare this definition (3.1) to the previous (1.1) and notice that now we do not postulate the linear interpolation. In this case, we only consider that the instantaneous payoff earned by players comes from the simultaneous participation in two games (one with each population) and we will obtain κ below as a result of the angular parametrization of these games.

Under standard assumptions for replicator dynamics, we can write the coupled system of ordinary differential equations as

$$\begin{cases} \dot{x} = x(1 - x)\Delta\pi_X \\ \dot{y} = y(1 - y)\Delta\pi_Y, \end{cases} \tag{3.2}$$

where $\Delta\pi_X = \pi_X(s_1; x, y) - \pi_X(s_2; x, y)$ is the fitness of strategy s_1 in population X, given the state of the system (x, y). Explicitly:

$$\Delta\pi_X = (\pi_{11}^A - \pi_{21}^A)\, x + (\pi_{12}^A - \pi_{22}^A)\,(1 - x) + (\pi_{11}^B - \pi_{21}^B)\, y + (\pi_{12}^B - \pi_{22}^B)\,(1 - y). \tag{3.3}$$

$\Delta\pi_Y$ is given by symmetry under the exchange of labels x and y. The growth rate of the strategies in each population is a function of the current state of the system (x, y) and of the entries of the two payoff matrices Π_A and Π_B. This is an autonomous system.

3.3 Angular representation of games[1]

In general two-strategy symmetric games of the form (Π, Π^T), the matrix Π introduces four degrees of freedom in the definition of the game: one per each element π_{ij}. Nevertheless, Π admits an angular parametrization such that only one degree

[1] This section presents a detailed derivation of the transformation required to find the angular parameter ϕ suggested in Szabó and Fáth, (2007).

of freedom is relevant for equilibrium predictions. This reduces the complexity of (3.2) and allows for a systematic analysis.

For any given Π, we can find a transformed matrix Π' that is equivalent to Π in the sense of the Nash equilibrium (NE) concept if $\Pi = \Pi' + C$ with

$$C = \begin{pmatrix} c_1 & c_2 \\ c_1 & c_2 \end{pmatrix}. \tag{3.4}$$

This addition of constants by columns preserves the original payoff comparison by rows. Straightforwardly, Π is also Nash-equivalent to Π' if we can write

$$\Pi = \alpha\big(\Pi' + C\big) \tag{3.5}$$

with α positive and finite.[2] The matrix $C = C(c_1, c_2)$ captures two of the degrees of freedom in Π, and the scalar α a third one. Then, Π' is constrained to have only one degree of freedom that we can denote by $\Pi' = \Pi'(\phi)$.

Setting α, c_1, and c_2 such that $\pi_{12} = \alpha c_2$ and $\pi_{21} = \alpha c_1$, we obtain Π' as a diagonal matrix. Because C is defined by columns and α is positive, we have

$$\frac{\pi_{22} - \pi_{12}}{\pi_{11} - \pi_{21}} = \frac{\pi'_{22}}{\pi'_{11}}. \tag{3.6}$$

This ratio between the diagonal elements of Π' can be parametrized by $\phi \in [0, 2\pi)$ with $\tan\phi = \pi'_{22}/\pi'_{11}$. Thus, there exists a transformation such that

$$\Pi = \begin{pmatrix} \pi_{11} & \pi_{12} \\ \pi_{21} & \pi_{22} \end{pmatrix} \sim_{\mathrm{NE}} \Pi' = \begin{pmatrix} \cos\phi & 0 \\ 0 & \sin\phi \end{pmatrix} \tag{3.7}$$

for any given Π. The angle ϕ encodes all the relevant information for the equilibrium analysis of the two-player game defined in the original payoff matrix Π.

We have defined above ϕ, c_1, and c_2 as functions of the elements in the original matrix Π. Solving explicitly for α in (3.5) with this information, we obtain the

[2] See Hofbauer and Sigmund, (1998, Section 11.2) for a general treatment of rescaled partnership games.

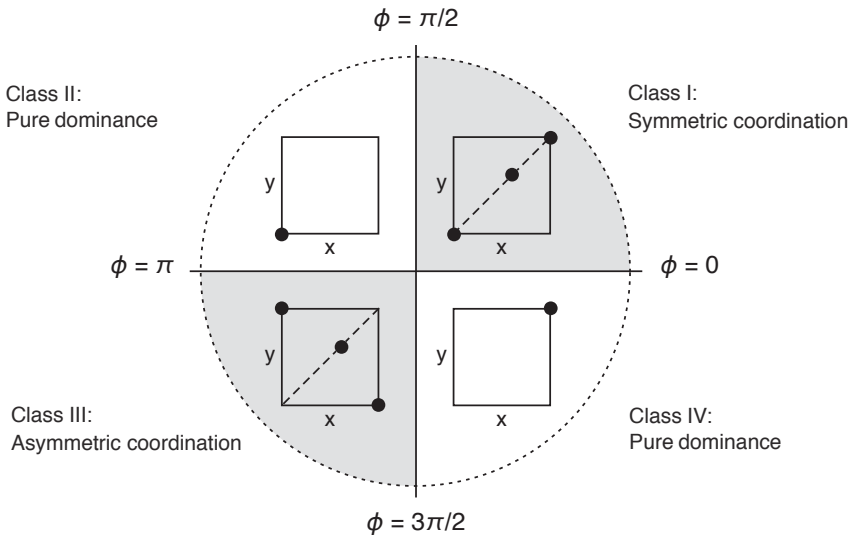

FIGURE 3.1: Classification of 2×2 symmetric games as a function of ϕ.

new parametrization in terms of the initial payoff entries that takes the form

$$\begin{cases} \phi &= \arctan\big[(\pi_{22} - \pi_{12})/(\pi_{11} - \pi_{21})\big] \\ c_1 &= \pi_{21}/\alpha \\ c_2 &= \pi_{12}/\alpha \\ \alpha^2 &= \pi_{11}(\pi_{11} - 2\pi_{21}) + \pi_{22}(1 - 2\pi_{12}) + \pi_{12}^2 + \pi_{21}^2. \end{cases} \tag{3.8}$$

Altogether, we obtain

$$\begin{pmatrix} \pi_{11} & \pi_{12} \\ \pi_{21} & \pi_{22} \end{pmatrix} = \alpha \left[\begin{pmatrix} \cos\phi & 0 \\ 0 & \sin\phi \end{pmatrix} + \begin{pmatrix} c_1 & c_2 \\ c_1 & c_2 \end{pmatrix} \right]. \tag{3.9}$$

It is well-known that 2×2 symmetric games can present at most three Nash equilibria (NE): two in pure strategies and one in symmetric mixed strategies. Figure 3.1 shows the classification of all possible 2×2 symmetric games depending on the set of NE that they present, as a function of the angular parameter ϕ (counterclockwise orientation). This taxonomy is concerned about the structure of the set of NE in the static version of the games. Later on, we will focus on the analysis of replicator dynamics to predict stability of the different configurations under the implementation with coupled populations; therefore, we avoid here any consideration about the strictness of the NE in the static context.

Class I: $\phi \in (0, \pi/2)$–symmetric coordination. This group presents two NE in pure strategies where both players coordinate either in action s_1 or in action s_2, and one symmetric NE in mixed strategies. In this case, both players randomize with a probability $x_{\mathrm{m}} = y_{\mathrm{m}} = 1/(1 + \cot\phi)$ of choosing s_1, which is increasing in ϕ.[3] When ϕ reaches the value of $\pi/2$, the mixed NE degenerates into the pure NE where both players coordinate in s_2. At this point, we find the transition to the second class of games.

Class II: $\phi \in (\pi/2, \pi)$–pure dominance (I). When ϕ crosses the boundary of $\pi/2$ coming from the previous class, the NE in which both players coordinate in action s_2 disappears and only coordination in action s_1 remains as a NE of the game. There is also no NE in mixed strategies. This class contains interactions in which one strategy exhibits pure dominance, such as the prisoner's dilemma. When $\phi = \pi$ the structure of the games changes and we find the transition to the third class of games.

Class III: $\phi \in (\pi, 3\pi/2)$–asymmetric coordination. When ϕ crosses the value of π, the unique NE of the previous class vanishes and two new asymmetric NE in pure strategies appear: players coordinate in opposite strategies. The previous symmetric NE in pure strategies is now transformed into a symmetric mixed NE that moves along the diagonal, once again with coordinates $x_{\mathrm{m}} = y_{\mathrm{m}} = 1/(1+\cot\phi)$ as in Class I. This class contains the hawk-dove game and related ones.

Class IV: $\phi \in (3\pi/2, 2\pi)$–pure dominance (II). When ϕ crosses $3\pi/2$, the symmetric mixed NE existing in the class of asymmetric coordination degenerates into a NE in pure strategies with coordination in action s_2. Class IV presents only this NE in pure strategies and is therefore equivalent to Class II under the exchange of labels s_1 and s_2.

This classification based on ϕ relates to the number of possible NE in the games and their type: mixed or pure; and in the second case, it also distinguishes asymmetric from symmetric cases. Cressman, (2003, Section 2.2) offers a similar taxonomy of games. More granularity can be obtained if one is concerned about other

[3] Computing the mixed NE in angular notation is almost trivial. Solving the mixing such that both pure strategies confronting the mixed one give the same expected payoff, $x_{\mathrm{m}} \cos\phi = (1 - x_{\mathrm{m}}) \sin\phi$; and solving for x_{m} we get $x_{\mathrm{m}} = 1/(1+\cot\phi)$, with derivative $\partial x_{\mathrm{m}}/\partial\phi = 1/(\cos\phi + \sin\phi)^2 > 0$.

Table 3.1: Baseline equilibria: static games and basic population structures

Game	(Static) NE	Replicator 1P	Replicator 2P
Class I: $\phi \in (0, \frac{\pi}{2})$	$\{(0,0), (1,1), (x_{\mathrm{m}}, y_{\mathrm{m}})\}$	$\{p_1, p_2, p_3, p_4\}$	$\{p_1, p_4\}$
Class II: $\phi \in (\frac{\pi}{2}, \pi)$	$\{(0,0)\}$	$\{p_1\}$	$\{p_1\}$
Class III: $\phi \in (\pi, \frac{3\pi}{2})$	$\{(0,1), (1,0), (x_{\mathrm{m}}, y_{\mathrm{m}})\}$	$\{p_9\}$	$\{p_2, p_3\}$
Class IV: $\phi \in (\frac{3\pi}{2}, 2\pi)$	$\{(1,1)\}$	$\{p_4\}$	$\{p_4\}$

with $x_{\mathrm{m}} = y_{\mathrm{m}} = 1/(1 + \cot\phi)$

properties. The notion of Pareto efficiency is not invariant under the relation of equivalence in the sense of the NE.[4]

Table 3.1 summarizes the angular classification of the different games that will be considered for the within- and between-group interactions, together with three baseline equilibrium predictions. First, we see the static Nash equilibria according to the discussion in the section above. When turning to the dynamic setting with standard replicator dynamics under one or two-population settings, we observe the first differences in how the population structure determines the dynamic stability of the different Nash equilibria.

For example, regarding Class I we see that under a one-population model, the only restriction is that the populations must be playing a pure strategy because every player within the group should make the same choice, and therefore any of the four corners of the phase space is compatible. Because in the two-population setting the logic is that both agents in the game (in this case players of opposing populations) will be playing the same action, then only the corners $(0,0)$ and $(1,1)$ are compatible. In plain words, we see that standard replicator dynamics provides two main results for equilibrium selection in coordination games: first, the mixed NE will never be selected either in one- or two-population settings; and second, the one-population setting is less demanding in that only within-group coordination is required (each group has to coordinate in one pure strategy, but it can be any of the two), while the two-population setting is more demanding if we interpret that these predictions require not only coordination within the group such that all agents are playing the same, but also impose a layer of coordination with the other group such that all players of the two groups are choosing the same.

[4]See Szabó and Fáth, (2007) also for a discussion about the complexity of classifying games with more than two strategies or with asymmetries.

Applied to Class III, we see that the story now is about specialization. The one-population setting does not allow for such an effect and therefore we only observe symmetric NE, but under a two-population setting, only the polarized configurations will be selected. Predictions about the pure dominance classes II and IV are independent of the population structure for obvious reasons. We now turn to study how these baseline predictions get enriched with the introduction of overlapping of the population structures.

3.4 Replicator dynamics

The fitness functions (3.3) have a linear dependency on the payoff structure of the games. They depend on payoff comparisons in the form $\pi^g_{1j} - \pi^g_{2j}$ with $j = 1, 2$ and $g = A, B$. Then, plugging the new parametrization of the payoff matrices (3.9) in the definition (3.3), we see that all terms that contain the constants c_1 and c_2 cancel out. We obtain the fitness function for strategy s_1 (in population X) as

$$\Delta\pi_X = \alpha_A\big[x\cos\phi_A - (1-x)\sin\phi_A\big] + \alpha_B\big[y\cos\phi_B - (1-y)\sin\phi_B\big]. \tag{3.10}$$

The corresponding formula for population Y comes by symmetry under the exchange of labels x and y, like in (3.3). Now, we have the dynamics of the system (3.2) depending on four parameters: two angular variables, ϕ_A and ϕ_B; and two scaling factors, α_A and α_B. Moreover, we can introduce the coupling parameter κ defined as

$$\kappa = \frac{\alpha_B}{\alpha_A + \alpha_B}. \tag{3.11}$$

The term $(\alpha_A + \alpha_B) > 0$ that would appear in the coupled system after rewriting (3.2) in terms of κ can be factored out with no concern. The equilibrium predictions of replicator dynamics are equivalent up to multiplicative (positive) constants. Then, the system (3.2) reduces to the following:

$$\begin{cases} \dot{x} &= x(1-x)\Big[(1-\kappa)\big[x\cos\phi_A - (1-x)\sin\phi_A\big] + \kappa\big[y\cos\phi_B - (1-y)\sin\phi_B\big]\Big] \\ \dot{y} &= y(1-y)\Big[(1-\kappa)\big[y\cos\phi_A - (1-y)\sin\phi_A\big] + \kappa\big[x\cos\phi_B - (1-x)\sin\phi_B\big]\Big]. \end{cases} \tag{3.12}$$

The triple $(\kappa,\ \phi_A,\ \phi_B)$ defines the complete family of replicator dynamics for 2×2 symmetric games with coupled populations. The coupling parameter κ takes

Table 3.2: Fixed points of replicator dynamics in (3.12)

Pure states	Hybrid states	Mixed states
$p_1 = \big(0,0\big)$	$p_5 = \big(0, [(1-\kappa)\sin\phi_A + k\sin\phi_B]/\Phi_h\big)$	$p_9 = \big(1/(1+\Phi_m), 1/(1+\Phi_m)\big)$
$p_2 = \big(1,0\big)$	$p_6 = \big(1, [(1-\kappa)\sin\phi_A - \kappa\cos\phi_B]/\Phi_h]\big)$	
$p_3 = \big(0,1\big)$	$p_7 = \big([(1-\kappa)\sin\phi_A + k\sin\phi_B]/\Phi_h, 0\big)$	
$p_4 = \big(1,1\big)$	$p_8 = \big([(1-\kappa)\sin\phi_A - \kappa\cos\phi_B]/\Phi_h], 1\big)$	

with $\Phi_h = (1-\kappa)(\cos\phi_A + \sin\phi_A)$
$\Phi_m = [(1-\kappa)\cos\phi_A + \kappa\cos\phi_B]/[(1-\kappa)\sin\phi_A + \kappa\sin\phi_B]$

values in the interval $[0,1]$ and measures the relative weight of the interaction between populations in the fitness function. The last transformation of the system of coupled differential equations with the introduction of (3.11) is not ill-defined unless both games have zero scaling factors, $\alpha_A + \alpha_B = 0$, a case in which the whole notion of payoff matrices as defined in (3.9) becomes meaningless. The angular parameters ϕ_A and ϕ_B take values in the interval $[0, 2\pi)$ and specify the class of each game class regarding static (Nash) equilibrium predictions (see Section above).

Table 3.2 reports the coordinates of the nine possible fixed points as functions of the three parameters (κ, ϕ_A, ϕ_B). In the Appendix A to this chapter, we solve for the location of the fixed points of (3.12), and conduct the linear stability analysis. In line with the analysis of the model in Chapter 1, there exist four fixed points corresponding to situations of pure play (the corners of the phase space), four hybrid states, and one symmetric mixed state. As one could expect from a generalization of the previous model, we now obtain six critical values of the coupling parameter κ that will play different roles in the existence and stability of the different possible fixed points. These elements depend on the angular parameters of the games, ϕ_A and ϕ_B, and will be relevant only if they belong to the interval $[0,1]$ by definition of the coupling parameter κ.

Table 3.3 shows the definition of the six critical values, $\{\kappa_n\}_{n=1}^{6}$. In particular, we have a subset of these critical values $\{\kappa_n\}_{i=1}^{4}$ that determines the conditions under which each of the possible fixed points exists (see Figure 3.6 in the Appendix A). The four values κ_n $(n \in \{1, \cdots, 4\})$ can be written in the form $1/(1+f_n)$ with these factors f_n defined as (± 1) a quotient of two trigonometric functions, sine or cosine. Existence of each critical threshold (understood as κ_n belonging to the unit interval) requires $f_n \geq 0$; and the sign of both sine and cosine functions is given by

TABLE 3.3: Critical values of κ

$\kappa_1(\phi_A, \phi_B) = \dfrac{1}{1 + \sin\phi_B / \cos\phi_A}$	$\kappa_4(\phi_A, \phi_B) = \dfrac{1}{1 - \cos\phi_B / \cos\phi_A}$
$\kappa_2(\phi_A, \phi_B) = \dfrac{1}{1 - \sin\phi_B / \sin\phi_A}$	$\kappa_5(\phi_A, \phi_B) = \dfrac{\cos\phi_A + \sin\phi_A}{\cos\phi_A + \cos\phi_B + \sin\phi_A + \sin\phi_B}$
$\kappa_3(\phi_A, \phi_B) = \dfrac{1}{1 + \cos\phi_B / \sin\phi_A}$	$\kappa_6(\phi_A, \phi_B) = \dfrac{\cos\phi_A + \sin\phi_A}{\cos\phi_A - \cos\phi_B + \sin\phi_A - \sin\phi_B}$

the quadrant of the angle. Therefore, the existence of each of these four critical values of the coupling parameter relates directly to the structure of four domains in the classification of games by their angular parameter ϕ. These four critical values, together with another two that are derived in the Appendix A as well, also determine the conditions for stability of the different fixed points (conditional on their existence, when required).

Regarding κ_5 and κ_6, their formulation is slightly more complex but still, one can see that such critical values will belong to $[0, 1]$ only for certain combinations of games (ϕ_A, ϕ_B). Explicitly, for the case of κ_5, we find these regions in the space of parameters to be $K_1(\kappa_5) = \{(\phi_A, \phi_B) \in [\frac{3\pi}{4}, \frac{7\pi}{4}] \times [\frac{3\pi}{4}, \frac{7\pi}{4}]\}$, $K_2(\kappa_5) = \{(\phi_A, \phi_B) \in [0, \frac{3\pi}{4}] \times [0, \frac{3\pi}{4}]\}$, $K_3(\kappa_5) = \{(\phi_A, \phi_B) \in [\frac{7\pi}{4}, 2\pi] \times [0, \frac{3\pi}{4}]\}$, $K_4(\kappa_5) = \{(\phi_A, \phi_B) \in [0, \frac{3\pi}{4}] \times [\frac{7\pi}{4}, 2\pi]\}$, and $K_5(\kappa_5) = \{(\phi_A, \phi_B) \in [\frac{7\pi}{4}, 2\pi] \times [\frac{7\pi}{4}, 2\pi]\}$. An equivalent analysis can be done for κ_6.

Altogether, different subsets of the six critical values of κ will play a role in determining the equilibrium predictions for different combinations of games (ϕ_A, ϕ_B). A graphical representation is the more suitable exposition.

Figure 3.2 takes the total two-dimensional space of parameters corresponding to all different pairs of angular definitions of the games, $[0, 2\pi] \times [0, 2\pi]$, and shows which critical values of κ can play a role under different combinations (ϕ_A, ϕ_B). First, we can see a basic orthogonal grid corresponding to steps of $\pi/2$ in both angles. These lines show the division of the different classes of games, $\{\mathrm{I}, \mathrm{II}, \mathrm{III}, \mathrm{IV}\}$, defined in Figure 3.1. Second, there is a finer set of boundaries that shows a tessellation such that in each tile, the existing values of critical κ maintain a particular order between them. These lines are analytically defined and there is no need for numerical solutions. To give the simplest example, the horizontal

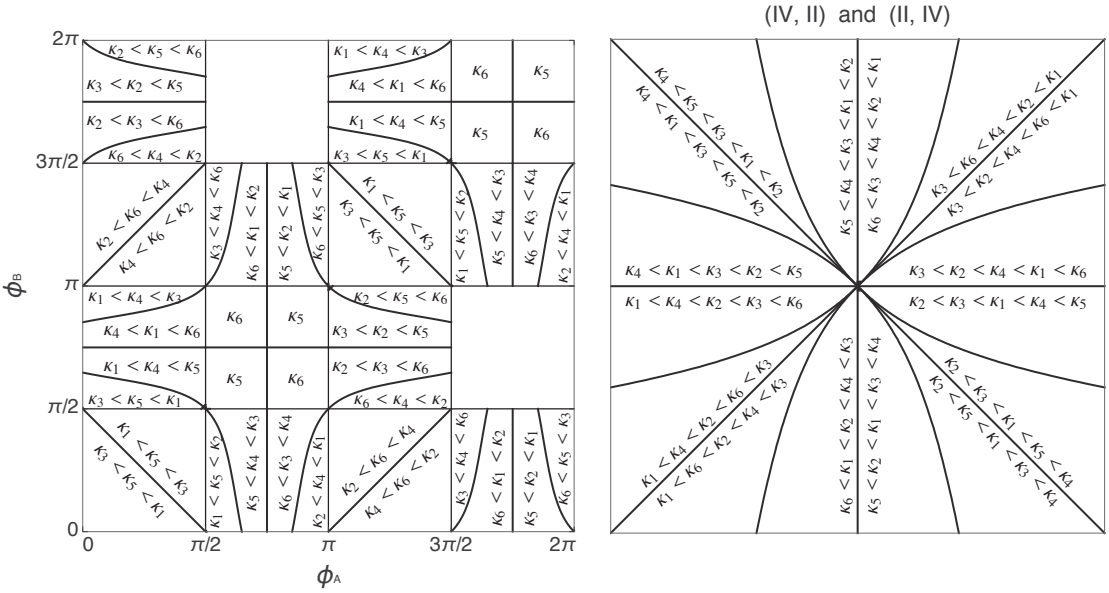

FIGURE 3.2: Relations among critical values of κ.

line running at a vertical coordinate of $\phi_B = 3\pi/4$ is given in implicit form as $\{(\phi_A, \phi_B) : \kappa_5(\phi_A, \phi_B) = \kappa_6(\phi_A, \phi_B)\}$, with κ_5 and κ_6 defined explicitly in Table 3.3. The rest of the lines are obtained by considering the different comparisons between the set of critical couplings, and we find eighty tiles in total.

Note that the right panel of Figure 3.2 shows the structure corresponding to the combinations (ϕ_A, ϕ_B) that belong to classes II and IV, or IV and II, equally. These two regions are equivalent to each other; they correspond to the coupling of games with pure dominance in opposing strategies, and one region can be obtained from the other one by reversing the labels in the action set. Interestingly enough, these combinations are the only ones where all six critical values of κ are present. The overlapping of the simplest strategic interactions can actually show the richest configurations for intermediate ranges of coupling.

The complexity introduced by this level of granularity in the space of parameters can be reduced when we focus on the equilibrium predictions. For each of these eighty tiles, we have found a sequence of critical levels of κ within the range $[0, 1]$ (remember Figure 3.2). In line with the study of the bifurcation in the hawk-dove game analyzed in Chapter 1, we can understand these sequences of critical values as candidates for bifurcation diagrams where κ is the bifurcation parameter. For the pairs of (ϕ_A, ϕ_B) within a particular tile, we study the effect of transiting from the one-population ($\kappa = 0$) to the two-population matching ($\kappa = 1$) in the linear

interpolation by increasing κ. In line with Section 1.3 of Chapter 1, we can find some of the thresholds to have a minor impact in the dynamics of the system, such as stability changes from source to saddle point with no major impact in terms of equilibrium predictions; but we will also find other thresholds to have a major impact shifting the stability conditions to qualitatively different configurations.

As an example of this, we focus now on the three lower tiles of the four that span the rectangle corresponding to the interaction of classes $\phi_A \in$ III (within-group) with $\phi_B \in$ II (between-groups) in Figure 3.2. These correspond to the sequences $0 < \kappa_2 < \kappa_6 < \kappa_3 < 1$, $0 < \kappa_2 < \kappa_3 < \kappa_6 < 1$, and $0 < \kappa_3 < \kappa_2 < \kappa_5 < 1$, respectively. Regarding equilibrium predictions, only κ_2 plays a role. As we will see illustrated later (discussion of the next Section, and diagram for region $\Phi^-_{\mathrm{III,II}}$ in Figure 3.4), we have the same scenario in the three tiles. First (for low levels of κ), the systems begins with the symmetric mixed equilibrium p_9 being the only attractor of the system. When κ increases, this p_9 approaches the corner p_1 with coordinates $(0, 0)$. At the point where the level of coupling reaches κ_2, this symmetric mixed point p_9 abandons the unit square through the corner $(0, 0)$, and the fixed point p_1 becomes the attractor of the dynamical system for values of $\kappa > \kappa_2$. Therefore, these three tiles correspond to the same qualitative bifurcation diagram: the system predicts always symmetric configurations, but stability shifts from an equilibrium in mixed strategies to an equilibrium in pure strategy s_2.

Going into more detail, at the same time as p_9 crosses p_1 ($\kappa \to \kappa_2$), the two hybrid points p_5 and p_7 do the same. Regarding, κ_3, this is the level of coupling for which the other two hybrid points p_6 and p_8 leave the unit square through the corners p_2 and p_3, which then change their (un-)stability properties from source to saddle point. The threshold κ_6 (or κ_5, depending on the case) is meaningless because it affects the sign of the eigenvalues of the symmetric mixed or the hybrid equilibria when they are already outside of the phase space (unit square).

We can conclude that the three tiles discussed in the paragraphs above actually correspond to the same class of dynamic predictions. There are only two regimes of equilibrium selection: symmetric mixed for $\kappa < \kappa_2$, and symmetric pure for $\kappa > \kappa_2$. The three tiles do not show qualitative differences in their bifurcation diagrams. Proceeding sequentially, we study the similarities between the predictions for the different eighty tiles, and see how they can be regrouped into only twenty-one.

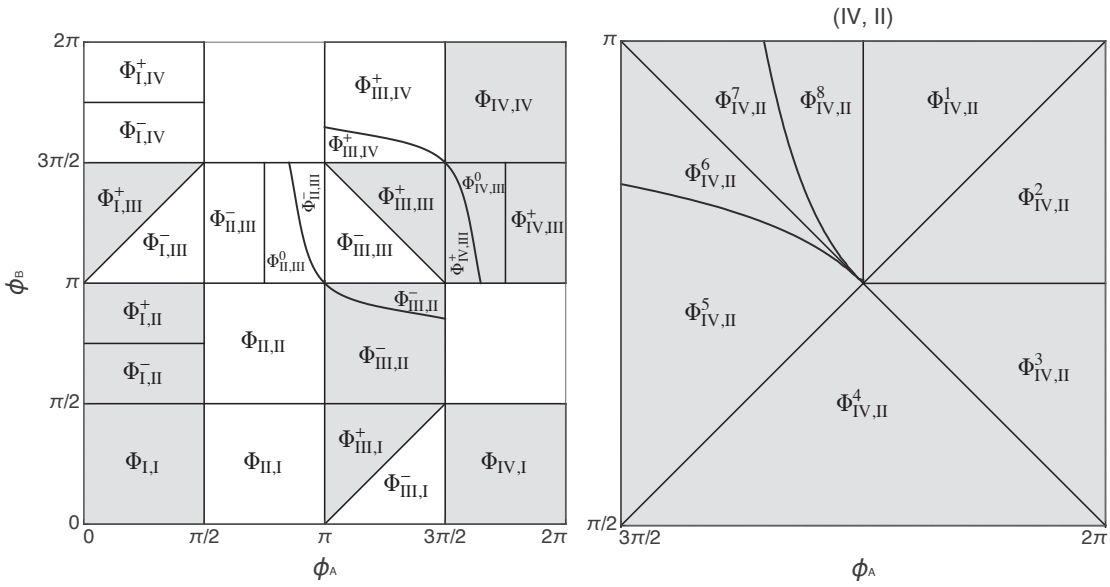

FIGURE 3.3: Regions of (ϕ_A, ϕ_B) grouping different bifurcations.

Figure 3.3 shows the classification of the regions in the parameter space (ϕ_A, ϕ_B) according to the regrouping of the tiles of Figure 3.2 as in the example discussed above. This grouping of the three tiles used to introduce this classification is now labeled as region $\Phi^{-}_{\mathrm{III,II}}$. The subindex III,II indicates that this region considers the coupling between games of Class III for the within-population interaction with games of Class II for the interaction between groups. The superindex $(-)$ in this case distinguishes this region from the neighboring $\Phi^{+}_{\mathrm{III,II}}$ which also considers games from the same classes, but restricted to a subset for which slightly different dynamics are predicted. Table 3.4 and Figure 3.4 complement Figure 3.3 and give a detailed explanation of all possible bifurcation scenarios that concern equilibrium selection with coupled populations in symmetric 2×2 games.

Two more aspects in Figure 3.3 deserve explanation. First, the shadowed areas select one of the (usually) two possible cases of each bifurcation scenario listed in Table 3.4. The next figure 3.4 illustrates these cases in more detail. See also the discussion below. Second, note that now, the detailed right panel of the figure only applies to the area corresponding to the coupling of Class IV with Class II while in Figure 3.2 the right panel was interchangeable for (IV, II) and (II, IV). When we analyze not only the relation among the critical values of κ but their equilibrium implications, we find that the bifurcations and dynamic predictions for the region (II, IV) are center-symmetric with respect to those of (IV, II). This is

not surprising, because Class IV and Class II are fully identical under the inversion of labels of the action set.

Table 3.4 in the Appendix B of this chapter shows the grouping of regions. These regions present qualitatively comparable dynamic predictions, except for some subtleties. We report twenty-one scenarios, but in all of the cases (except in scenario 1) we see that each scenario comprises two regions. As a first example, let us focus on scenario 13 that contains regions $\Phi^{+}_{\mathrm{III,III}}$ and $\Phi^{-}_{\mathrm{III,III}}$. This scenario contains the hawk-dove model studied in Chapter 1. The experimental payoff matrix (1.5) sets $\phi_A = \phi_B = \arctan 2 - \pi$, a configuration that belongs to the region $\Phi^{+}_{\mathrm{III,III}}$. The intermediate regime of equilibrium selection is such that p_6 and p_8 are the possible attractors. If we considered the case of region $\Phi^{-}_{\mathrm{III,III}}$ we would obtain the intermediate regime to be with p_5 and p_7 as attractors.

Both regions present the same bifurcation diagram, up to the usual exchange of labels in the action set. A similar logic applies for the rest of paired regions that exhibit the same bifurcation scenarios. We illustrate a representative example of each reagion with a bifurcation diagram showing the different regimes of equilibrium selection in Figure 3.4 and explain them briefly in Section 3.6 where we also compare them with their respective counterparts with perturbed best response dynamics.

The following Proposition 3.1 summarizes the results obtained for the general model of replicator dynamics with coupled populations (3.2). Its structure is similar to the one in Chapter 1 but with a slightly more complex formulation because Proposition 1.1 is only a particularly simple subcase of the more general Proposition 3.1.

Proposition 3.1. *Given the coupled system of replicator dynamics in (3.12) and for every pair of games* $(\phi_A, \phi_B) \in [0, 2\pi) \times [0, 2\pi)$*, there exist two critical values of the coupling parameter* $\kappa^*_{1P} \leq \kappa^*_{2P}$ *that belong to the interval* $(0, 1)$*, and such that:*

(a) if $\kappa < \kappa^*_{1P}$*, the equilibrium will be as in the one-population model with the game determined by* ϕ_A*,*

(b) if $\kappa > \kappa^*_{2P}$*, the equilibrium will be as in the two-population model with the game determined by* ϕ_B*,*

(c) if $\kappa \in (\kappa^*_{1P}, \kappa^*_{2P})$*, the equilibrium will be qualitatively different from the standard one- and two-population models.*

Table 3.4 (in the Appendix B to this chapter) gives the cutoff points κ^*_{1P} *and* κ^*_{1P} *for different combinations of* (ϕ_A, ϕ_B) *in terms of the critical values of* κ *defined in Table 3.3. There are twenty-one different scenarios (in Table 3.3) that can be classified according to the complexity of their intermediate regime:*

1. *No intermediate regime (4 scenarios):*[5] *1, 5, 6, and 11.*
2. *Simple intermediate regime (10):*[6] *2, 3, 4, 7, 8, 10, 12, 13, 17, and 18.*
3. *Intermediate regime containing two subregimes (2): 9, and 19.*
4. *Intermediate regime containing three subregimes (4): 14, 15, 16, and 21.*
5. *Intermediate regime containing four subregimes: 20.*

[5]Cases where case (c) above is void
[6]Cases comparable to the study in Chapter 1

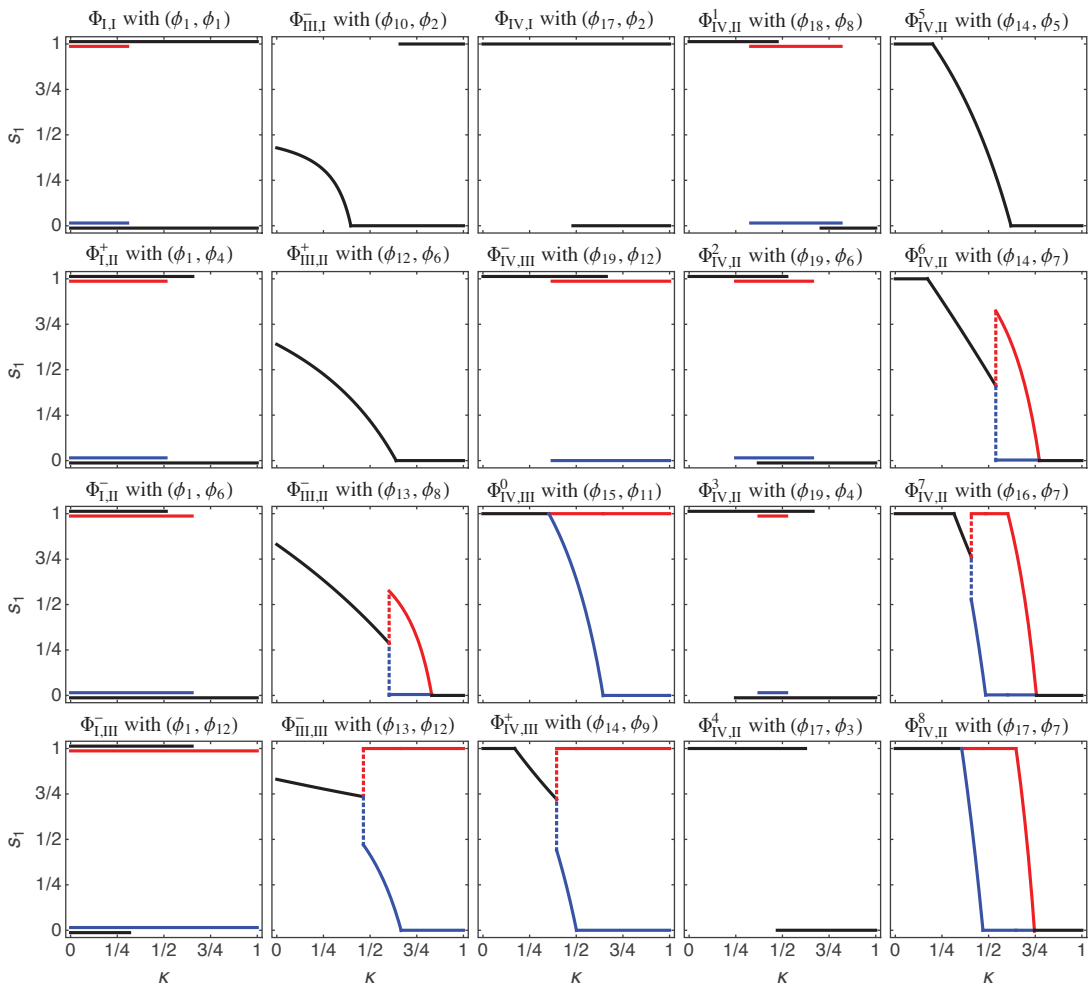

FIGURE 3.4: Bifurcations predicted by replicator dynamics.
(Numerical values of the different angles in Table 3.5, Appendix B.)

3.5 PBR dynamics

We follow the definition of the model for PBR dynamics employed in Chapter 2 and apply it to the general case of coupled populations that we have explained in the Section above. Therefore, we consider a system of the form

$$\begin{cases} \dot{x} &= p_X(s_1;\, x, y) - x \\ \dot{y} &= p_Y(s_1;\, x, y) - y, \end{cases} \tag{3.13}$$

where p_X is given by

$$p_X(s_1;\, x, y) = \frac{1}{1 + e^{-\lambda \Delta\pi_X(x,y)}}, \tag{3.14}$$

and p_Y is defined analogous (given the symmetry of the system). The term $\Delta\pi_X(x, y)$ is the fitness function as already defined in Chapters 1 and 2, $\Delta\pi_X(x, y) = \pi_X(s_1;\, x, y) - \pi_X(s_2;\, x, y)$, with

$$\pi_X(s_i;\, x, y) = (1 - \kappa)[\pi_{i1}x + \pi_{i2}(1 - x)] + \kappa[\pi_{i1}y + \pi_{i2}(1 - y)]. \tag{3.15}$$

This is slightly different from (3.10) because the predictions with PBR dynamics are not fully invariant under the transformation defined in (3.9), as opposed to replicator dynamics. As usual, λ can be interpreted dually as a rationality exponent or also as the inverse of the noise in the system. When $\lambda = 0$, the selection of actions by the players is independent of the payoff structure of the game and the systems evolve toward an equal share of strategies. When $\lambda \to \infty$, the system approaches replicator dynamics.

Due to the presence of the exponential function combined with the linear term, there is no closed form solution to (3.13). We briefly explore the general PBR system numerically. This provides some behavioral insights to complement the replicator predictions. Figure 3.5 mirrors the structure of one example per region as in Figure 3.4 to allow for comparison (solutions are plotted with $\lambda = 2$).

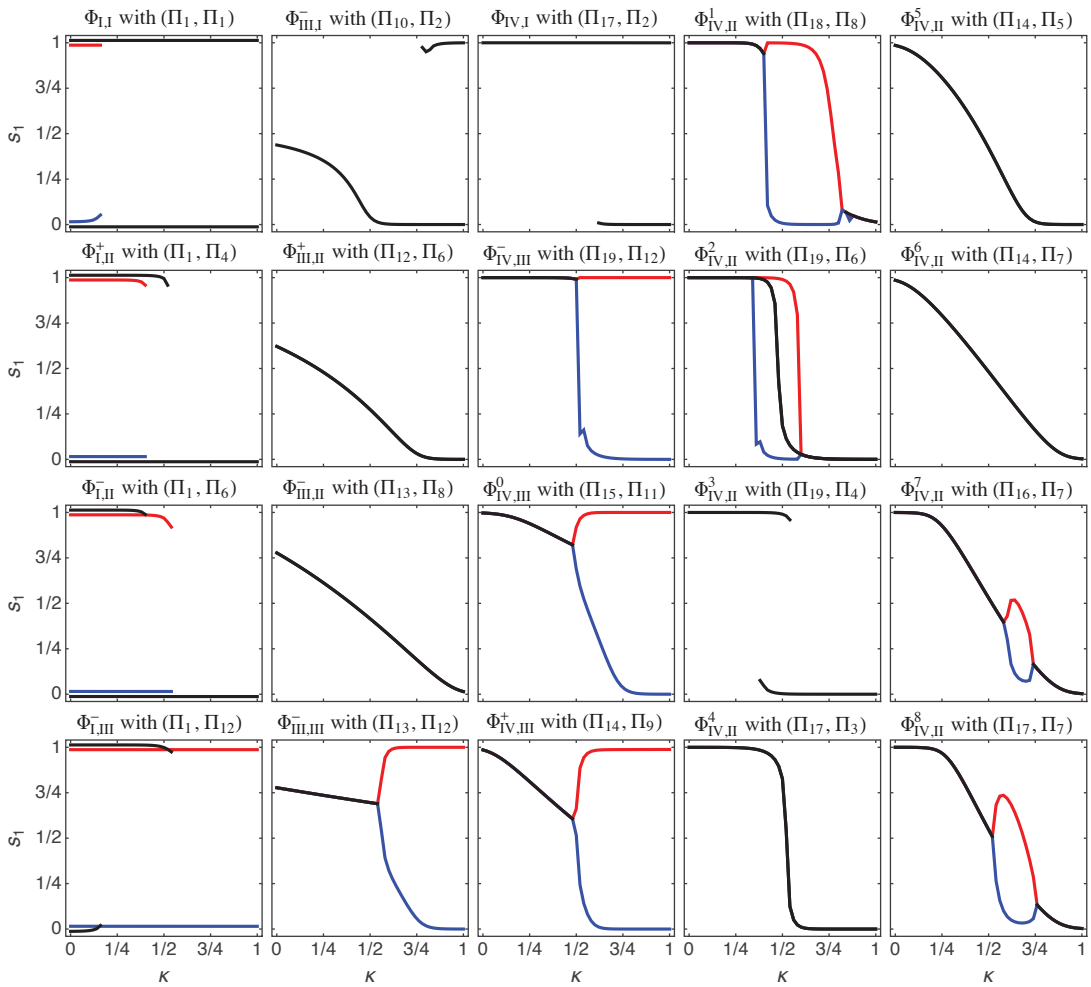

FIGURE 3.5: Solutions with PBR dynamics.
(Entries of the different payoff matrices in Table 3.6, Appendix B.)

3.6 Scenarios of equilibrium predictions

The purpose of analyzing the general models of replicator and PBR dynamics with coupled populations for any possible pair of games Π_A and Π_B is to establish a set of evolutionary predictions regarding the equilibrium selection for this family of interactions. Table 3.4 and Figures 3.4 and 3.5 summarize the analysis performed in this chapter. Before concluding, we describe here the different scenarios that have been computed with replicator dynamics and comment on the behavioral variations that we can expect from the insights brought about by the PBR model.

Scenario 1 is the only simple case containing a unique region ($\Phi_{\mathrm{I,I}}$) corresponding to the coupling of two coordination games. There are two regimes of equilibrium selection with κ_1 as the critical value. For lower values $\kappa < \kappa_1$, the four corners $\{p_i\}_{i=1}^4$ are attractors of the system. This is the one-population prediction where each of the two populations can coordinate in their own strategy, but the strategies of the two populations are independent of each other. For higher values $\kappa > \kappa_1$, only the two symmetric corners p_1 and p_4 are attractors. This is the two-population prediction where the two populations coordinate in the same strategy. In this case, the effect of a sufficient coupling is to impose full symmetry in the system: players will align their choices at two levels: with their own group and with the other one.

Scenario 2: Region $\Phi^+_{\mathrm{I,II}}$ (and $\Phi^-_{\mathrm{I,IV}}$) corresponding to the coupling of a coordination game within the groups and a pure dominance game between the groups. There are three regimes of equilibrium selection with κ_4 and κ_1 (or κ_2 and κ_3) as critical values. For lower values $\kappa < \kappa_4$ (or $\kappa < \kappa_2$), the four corners $\{p_i\}_{i=1}^4$ are attractors of the system, as above. For higher values $\kappa > \kappa_1$ (or $\kappa > \kappa_3$), only the symmetric corner p_1 (or p_4) is attractor. This is the two-population prediction where the two groups coordinate in the dominant strategy. For the intermediate range $\kappa_4 < \kappa < \kappa_1$ (or $\kappa_2 < \kappa < \kappa_3$), three points are attractors: the two polarized ones and the one corresponding to coordination in the dominant strategy. In this case, the effect of the introduction of coupling is first to eliminate the attractor in which both populations would coordinate in the dominated strategy and then to eliminate the polarized cases.

Scenario 3: Region $\Phi^-_{\mathrm{I,II}}$ (and $\Phi^+_{\mathrm{I,IV}}$) corresponding as well to the coupling of a coordination game within the groups and a pure dominance game between the groups. There are three regimes of equilibrium selection with κ_1 and κ_4 (or κ_3

and κ_2) as critical values. For lower values $\kappa < \kappa_1$ (or $\kappa < \kappa_3$), the four corners $\{p_i\}_{i=1}^4$ are attractors of the system, as above. For higher values $\kappa > \kappa_4$ (or $\kappa > \kappa_2$), only the symmetric corner p_1 (or p_4) is attractor, for the same reason as above. For the intermediate range $\kappa_1 < \kappa < \kappa_4$ (or $\kappa_3 < \kappa < \kappa_2$), two points are attractors: the two symmetric ones. Therefore, in this case (and a difference with respect to the case above) the effect of increasing the coupling is first to eliminate the polarized configuration and then to eliminate the symmetric configuration that is not compatible with the game between populations.

Scenario 4: Region $\Phi^+_{\mathrm{I,III}}$ (and $\Phi^-_{\mathrm{I,III}}$) corresponding to the coupling of a coordination game within the groups and an asymmetric coordination game between the groups. There are three regimes of equilibrium selection with κ_2 and κ_4 (or κ_4 and κ_2) as critical values. For lower values $\kappa < \kappa_2$ (or $\kappa < \kappa_4$), the four corners $\{p_i\}_{i=1}^4$ are attractors of the system, as above. For higher values $\kappa > \kappa_4$ (or $\kappa > \kappa_2$), only the asymmetric corners p_2 and p_3 are attractors. For the intermediate range $\kappa_2 < \kappa < \kappa_4$ (or $\kappa_4 < \kappa < \kappa_2$), three points are attractors: the two asymmetric ones and a symmetric one, p_4 (or p_2). In this case, the effect of increasing the coupling is to eliminate the symmetric configurations in a sequential manner, until the only remaining attractors are compatible with the asymmetry induced by the coupling between groups.

In these four scenarios containing the coordination games as the interaction within the groups, the introduction of noise with the PBR model shifts down the critical values of κ defining the different regimes. Thus, the presence of noise makes the one-population prediction of replicator dynamics when the home game is a coordination game less robust against perturbations from coupling with the other group.

Scenario 5: Region $\Phi_{\mathrm{II,I}}$ (and $\Phi_{\mathrm{IV,I}}$) corresponding to the coupling of a pure dominance game within the groups and a coordination game between the groups. There are two regimes of equilibrium selection with κ_4 (or κ_2) as critical values. For lower values $\kappa < \kappa_4$ (or $\kappa < \kappa_2$), the only attractor is the symmetric corner p_1 (or p_4) as one could expect from the one-population model. For higher values $\kappa > \kappa_4$ (or $\kappa > \kappa_2$), there exist the two symmetric attractors p_1 and p_4. In this case, the effect of increasing the coupling is first to introduce the remaining symmetric configuration in a sequential manner.

Scenario 6: Region $\Phi_{\mathrm{II,II}}$ (and $\Phi_{\mathrm{IV,IV}}$) corresponding to the coupling of two pure dominance games within the groups and between the groups, with the same action being the dominant one in both interactions. There is a unique regime ($0 < \kappa < 1$) such that the corner with symmetric configuration in the dominant action is the only attractor (p_1 or p_4, respectively).

Scenario 7: Region $\Phi^{-}_{\mathrm{II,III}}$ (and $\Phi^{+}_{\mathrm{IV,III}}$) corresponding to the coupling of a pure dominance game within the groups and an asymmetric coordination game between the two populations. There are three regimes of equilibrium selection with κ_1 and κ_2 (or κ_3 and κ_4) as critical values. For lower values $\kappa < \kappa_1$ (or $\kappa < \kappa_3$), the only attractor is the symmetric corner p_1 (or p_4) as one could expect from the one-population model. For higher values $\kappa > \kappa_2$ (or $\kappa > \kappa_4$), there exist the two asymmetric attractors p_2 and p_3 corresponding to the two-population case. In the intermediate regime $\kappa_1 < \kappa < \kappa_2$ (or $\kappa_3 < \kappa < \kappa_4$), the three attractors (either p_1, p_2, p_3 or p_2, p_3, p_4) coexist.

Scenario 8: Region $\Phi^{0}_{\mathrm{II,III}}$ (and $\Phi^{0}_{\mathrm{IV,III}}$) corresponding to the coupling of a pure dominance game within the groups and an asymmetric coordination game between the two populations. There are three regimes of equilibrium selection with κ_2 and κ_1 (or κ_4 and κ_3) as critical values. For the lower and higher values of κ the logic is as described above, and the difference with respect to scenario 7 is that now the intermediate regime has the hybrid points p_5 and p_7 (or p_6 and p_8) as attractors. In this case, the transition from symmetric pure play to asymmetric pure play is through these points in which one group moves from one strategy to the other one in a continuous manner.

Scenario 9: Region $\Phi^{+}_{\mathrm{II,III}}$ (and $\Phi^{-}_{\mathrm{IV,III}}$) corresponding to the coupling of a pure dominance game within the groups and an asymmetric coordination game between the two populations. There are four regimes of equilibrium selection, as a minor difference with respect to the previous scenario. The sequence of critical values of κ is κ_2, κ_5, κ_1 (or κ_4, κ_5, κ_3). The first, third, and fourth regime occur as above, and the novelty is the presence of a second regime for $\kappa_2 < \kappa < \kappa_5$ (or $\kappa_4 < \kappa < \kappa_5$) in which the attractor is the symmetric mixed point.

In all these cases containig the pure dominance game as the within-group game, the PBR model considering the presence of behavioral noise extends the domain of κ for which the one-population prediction holds qualitatively, usually reducing

the scope of the two-population predictions. In the subcases where the system evolves toward separation for high values of coupling, the transition occurs in a smooth way, analogous to the analysis performed in Chapter 2. In general, PBR also smoothens the transition from symmetric pure play to symmetric mixed play, as we can see in the PBR diagrams for scenario 9.

Scenario 10: Region $\Phi^{+}_{\mathrm{III,I}}$ (and $\Phi^{-}_{\mathrm{III,I}}$) corresponding to the coupling of an asymmetric coordination game as the within-group interaction and a symmetric coordination game between the groups. There are three regimes of equilibrium selection with κ_2 and κ_4 (or κ_4 and κ_2) as critical values. For the lower values $\kappa < \kappa_2$ (or $\kappa < \kappa_4$), the symmetric mixed point is the only attractor of the system. This point moves toward the symmetric pure point p_1 (or p_4) that is the only attractor in the intermediate regime $\kappa_2 < \kappa < \kappa_4$ (or $\kappa_4 < \kappa < \kappa_2$). For high values $\kappa > \kappa_4$ (or $\kappa > \kappa_2$), a second attractor is present: the remaining symmetric pure configuration p_4 (or p_1).

The effect of the introduction of noise in this scenario with PBR dynamics is to smoothen the S-shape of the transition from the mixed to the pure solution, and to decrease the scope of the two-population prediction with the two symmetric solutions.

Scenario 11: Region $\Phi^{-}_{\mathrm{III,II}}$ (and $\Phi^{+}_{\mathrm{III,IV}}$) corresponding to the coupling of an asymmetric coordination game as the within-group interaction and a pure dominance game between the groups. There are two regimes of equilibrium selection in this case, with κ_2 (or κ_4) as the only critical value of coupling. We observe a direct transition from the one-population to the two-population prediction through the movement of the symmetric mixed equilibrium toward the corresponding corner of the symmetric pure configuration p_1 (or p_4).

In line with the case above, the effect of the behavioral noise is to smoothen the S-shape of the transition.

Scenario 12: Region $\Phi^{+}_{\mathrm{III,II}}$ (and $\Phi^{-}_{\mathrm{III,IV}}$) is quite similar to scenario 11 but now, there are three regimes of equilibrium selection with critical values κ_5 and κ_2 (or κ_5 and κ_4). The intermediate regime that we can find in this case introduces a minor and subtle difference with respect to scenario 11: the transition occurs through the hybrid configuration, such that one group moves to the pure play earlier (for lower values of coupling) than the other one.

This "bubble" vanishes with the introduction of regular levels of behavioral noise in the PBR model.

Scenario 13: Region $\Phi^{-}_{\mathrm{III,III}}$ (and $\Phi^{+}_{\mathrm{III,III}}$) corresponding to the coupling of two (generally different) asymmetric coordination games as both the within- and the between-group interaction. There are two critical values of κ which are κ_5 and κ_1 (or κ_5 and κ_3), and the structure of the regimes for equilibrium selection is quite similar to the one described in scenario 12, except that now, the two-population prediction is a polarized asymmetric attractor.

The effect of introducing noise with the PBR model is that the symmetric mixed equilibrium extends for longer overlap, decreasing the scope of the two-population prediction, and of course, the transition predicted via the hybrid points is smoother and without kinks.

As stated in Table 3.4, *Scenarios 14-21* correspond to the coupling of two games of pure dominance in opposed strategies and show very intricate sequences of possible attractors (Figure 3.4, columns 4-5); however, we can describe them intuitively by regrouping them according to the refinement in the predictions given by PBR dynamics in Figure 3.5 (columns 4-5 as well).

The four scenarios of column 4 (Figure 3.4) show cases where there is a transition from the one-population to the two-population prediction via an overlapping of all possible corners where pure strategies are played. The different scenarios differ in the way in which different attractors overlap. Column 5 shows the cases where the transition regime occurs along a situation (or possibly several) of unique predictions, ranging from a simple transition following the moving symmetric attractor, or through the polarized and hybrid cases. PBR allows us to classify the expected behavior into two broad groups: (a) almost trivial situations where we observe an S-curve such that the transition from one pure play to the opposite one is smooth and the symmetry of the system is never broken (although scenario 16 is more complex because the system shows hysteresis); (b) a variation of case (a) such that a "bubble" can appear depending on the level of noise which is reminiscent of the presence of polarized and hybrid attractors in replicator dynamics. Scenario 15 contains both types of predictions.

3.7 Conclusion

This chapter presented a thorough and systematic generalization of the ideas introduced theoretically and experimentally in Chapter 1 and further analyzed in Chapter 2. The initial model (Benndorf et al., 2016) considered only an interpolation between the one-population and the two-population matching protocols of the same game of the hawk-dove type. Here, we considered the coupled model in general terms, allowing for any pair of possibly different games. The analysis was simplified by introducing a minimal set of parameters that represent all relevant degrees of freedom of the dynamical system, given the best-response paradigm. We also showed that the parameter κ defining the linear interpolation between the two matching protocols can be defined naturally in terms of the scaling parameters of the games in angular notation.

Moreover, the parametrization that we employ allowed us to systematically classify all possible evolutionary scenarios that can occur under replicator dynamics when any pair of symmetric 2×2 games overlap. There exist twenty-one different analytical scenarios for replicator dynamics, and these can be reduced to four families of behavioral patterns according to perturbed best response dynamics. The first group contains those situations where a coordination game plays the role of the within-group interaction. In these cases, obtain different sequences of equilibria in pure strategies. The second family groups situations where we expect S-shaped patterns (sometimes starting directly in a mixed situation and not only in pure strategies) such that the system changes the mixing of strategies depending on the coupling, but the symmetry is never broken. We can define the third group as those bifurcations exhibiting a "fork" shape such that the system presents symmetric states in the vicinity of the one-population model, and transit to polarized states in close to the two-population matching protocol. The fourth group shows the S-pattern characteristic from the second family, together with an intermediate regime with the shape of a "bubble" such that there exist moderate levels of coupling for which the groups polarize in their behavior, even though the system exhibits symmetry in the neighborhood of the one- and two-population cases. These results pave the ground for a further experimental agenda.

Appendix A - Linear stability analysis

Coordinates of the fixed points

From the replicator dynamics (3.12) we obtain the zero-growth lines:

$$\begin{aligned} \dot{x} = 0 \rightarrow & \begin{cases} x = 0 \\ x = 1 \\ x = \dfrac{(1-\kappa)\sin\phi_A - \kappa\, y \cos\phi_B + \kappa(1-y)\sin\phi_B}{(1-\kappa)(\cos\phi_A + \sin\phi_A)} \end{cases} \\ \dot{y} = 0 \rightarrow & \begin{cases} y = 0 \\ y = 1 \\ y = \dfrac{(1-\kappa)\sin\phi_A - \kappa\, x \cos\phi_B + \kappa(1-x)\sin\phi_B}{(1-\kappa)(\cos\phi_A + \sin\phi_A)}. \end{cases} \end{aligned} \tag{3.16}$$

Intersections of two nullclines (one of zero horizontal velocity and one of zero vertical velocity) determine the location of the possible fixed points. The first four points are trivial to obtain and correspond to the corners of the phase space. These points represent possible equilibria in which both populations play pure strategies:

$$p_1 = (0,0),\ p_2 = (1,0),\ p_3 = (0,1),\ p_4 = (1,1). \tag{3.17}$$

Other four possible fixed points move along the four edges of the phase space and describe hybrid states (one population plays a pure strategy and the other mixes):

$$\begin{aligned} p_5 &= \left(0,\ \left[(1-\kappa)\sin\phi_A + \kappa\sin\phi_B\right]/\Phi_h\right), \quad p_6 = \left(1,\ \left[(1-\kappa)\sin\phi_A - \kappa\cos\phi_B\right]/\Phi_h\right), \\ p_7 &= \left(\left[(1-\kappa)\sin\phi_A + \kappa\sin\phi_B\right]/\Phi_h,\ 0\right), \quad p_8 = \left(\left[(1-\kappa)\sin\phi_A - \kappa\cos\phi_B\right]/\Phi_h,\ 1\right), \end{aligned} \tag{3.18}$$

with $\Phi_h = (1-\kappa)(\cos\phi_A + \sin\phi_A)$. The final possible fixed point is the interior solution in which both populations play symmetric mixed strategies:

$$p_9 = \left(\frac{1}{1+\Phi_m}, \frac{1}{1+\Phi_m}\right) \text{ with } \Phi_m = \frac{(1-\kappa)\cos\phi_A + \kappa\cos\phi_B}{(1-\kappa)\sin\phi_A + \kappa\sin\phi_B}. \tag{3.19}$$

Points 1 to 4 always belong to the square of unit side, by definition. The four hybrid cases 5 to 8 can be grouped by pairs depending on their common existence conditions. Points p_5 and p_7 exist if and only if

$$0 \leq \frac{1}{\Phi_h}\left[(1-\kappa)\sin\phi_A + \kappa\sin\phi_B\right] \leq 1. \tag{3.20}$$

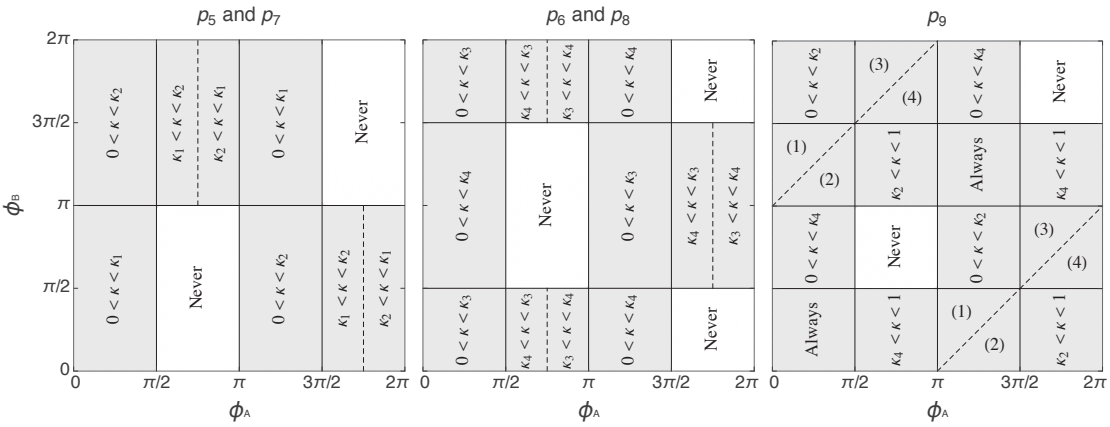

FIGURE 3.6: Conditions on κ for the existence of the hybrid and mixed states for all possible combinations of games. The four smaller regions: (1) $0 < \kappa < \kappa_2 \cup \kappa_4 < \kappa < 1$, (2) $0 < \kappa < \kappa_4 \cup \kappa_2 < \kappa < 1$, (3) $\kappa_4 < \kappa < \kappa_2$, and (4) $\kappa_2 < \kappa < \kappa_4$.

The values of κ for which the two inequalities in (3.20) become equalities (independently) give two critical values of the coupling parameter,

$$\kappa_1(\phi_A, \phi_B) = \frac{1}{1 + \sin\phi_B / \cos\phi_A} \quad \text{and} \quad \kappa_2(\phi_A, \phi_B) = \frac{1}{1 - \sin\phi_B / \sin\phi_A}. \tag{3.21}$$

Points p_6 and p_8 exist if and only if

$$0 \leq \frac{1}{\Phi_h}\big[(1-\kappa)\sin\phi_A + \kappa \sin\phi_B\big] \leq 1, \tag{3.22}$$

and in this case we obtain

$$\kappa_3(\phi_A, \phi_B) = \frac{1}{1 + \cos\phi_B / \sin\phi_A} \quad \text{and} \quad \kappa_4(\phi_A, \phi_B) = \frac{1}{1 - \cos\phi_B / \cos\phi_A}. \tag{3.23}$$

Point p_9 belongs to $[0,1] \times [0,1]$ if and only if $\Phi_m \geq 0$. Because Φ_m is a fraction, this condition is satisfied only when numerator and denominator have the same sign. One can check that the critical values of κ for which the numerator and the denominator equal to zero are κ_4 and κ_2, respectively.

Given these boundaries that we have computed, $\{\kappa_n\}_{n=1}^4$, we show in Figure 3.6 the conditions for existence of the points with moving coordinates in the different regions of the space of parameters.

Eigenvalues of the fixed points

Stability of the fixed points comes determined by the sign of the eigenvalues of the Jacobian matrix, J, evaluated at each point's coordinates. We look for the conditions under which both eigenvalues of J (evaluated at the point's coordinates) are negative (Hofbauer and Sigmund, 2003); and these eigenvalues, ν_1 and ν_2, are the two roots of the characteristic polynomial $\det\left[\nu\mathbb{I}_2 - J\right]$. The Jacobian matrix has its elements $J_{mn} = \partial\dot{m}/\partial n$ given by

$$\begin{aligned} J_{xx} &= (2-3x)x(1-\kappa)\cos\phi_A - (1-3x)(1-x)(1-\kappa)\sin\phi_A \\ &\quad + (1-2x)\kappa\left[y\cos\phi_B - (1-y)\sin\phi_B\right], \\ J_{xy} &= (1-x)x\kappa(\cos\phi_B + \sin\phi_B); \end{aligned} \tag{3.24}$$

with J_{yx} and J_{yy} given by symmetry under the exchange of variables x and y. Solving for $\nu_1(p_i)$ and $\nu_2(p_i)$ where $p_i = (x_i, y_i)$, and $i = 1, \ldots, 9$ covers the set of fixed points, we obtain the corresponding eigenvalues according to

$$\begin{aligned} \nu_1(p_1) &= \nu_2(p_1) = -(1-\kappa)\sin\phi_A - \kappa\sin\phi_B, \\ \nu_1(p_2) &= \nu_1(p_3) = -(1-\kappa)\sin\phi_A + \kappa\cos\phi_B, \\ \nu_2(p_2) &= \nu_2(p_3) = -(1-\kappa)\cos\phi_A + \kappa\sin\phi_B, \\ \nu_1(p_4) &= \nu_2(p_4) = -(1-\kappa)\cos\phi_A - \kappa\cos\phi_B, \\ \nu_1(p_5) &= \nu_1(p_7) = \left[(\cos\phi_A - \kappa\cos\phi_A - \kappa\sin\phi_B)^{-1} + (\sin\phi_A - \kappa\sin\phi_A + \kappa\sin\phi_B)^{-1}\right]^{-1}, \\ \nu_2(p_5) &= \nu_2(p_7) = \left[\kappa(\cos\phi_B + \sin\phi_B) - (1-\kappa)(\cos\phi_A + \sin\phi_A)\right] \\ &\qquad \times\left[(1-\kappa)\sin\phi_A + \kappa\sin\phi_B\right]\left[(1-\kappa)(\cos\phi_A + \sin\phi_A)\right]^{-1}, \\ \nu_1(p_6) &= \nu_1(p_8) = \left[(1-\kappa)\cos\phi_A + \kappa\cos\phi_B\right]\left[(1-\kappa)\sin\phi_A - \kappa\cos\phi_B\right] \\ &\qquad \times\left[(1-\kappa)(\cos\phi_A + \sin\phi_A)\right]^{-1}, \\ \nu_2(p_6) &= \nu_2(p_8) = \left[\kappa(\cos\phi_B + \sin\phi_B) - (1-\kappa)(\cos\phi_A + \sin\phi_A)\right] \\ &\qquad \times\left[(1-\kappa)\cos\phi_A + \kappa\cos\phi_B\right]\left[(1-\kappa)(\cos\phi_A + \sin\phi_A)\right]^{-1}, \\ \nu_1(p_9) &= \left[(1-\kappa)\cos\phi_A + \kappa\cos\phi_B\right]\left[(1-\kappa)(\cos\phi_A + \sin\phi_A) - \kappa(\cos\phi_B + \sin\phi_B)\right] \\ &\qquad \times\left[(1-\kappa)\sin\phi_A + \kappa\sin\phi_B\right]\left[(1-\kappa)(\cos\phi_A + \sin\phi_A) + \kappa(\cos\phi_B + \sin\phi_B)\right]^{-2}, \\ \nu_2(p_9) &= \left[(\cos\phi_A - \kappa\cos\phi_A + \kappa\cos\phi_B)^{-1} + (\sin\phi_A - \kappa\sin\phi_A + \kappa\sin\phi_B)^{-1}\right]^{-1}. \end{aligned} \tag{3.25}$$

Note that in order to determine the range of parameters for which a fixed point p_i is an attractor of the dynamical system, and therefore likely to be selected as

an equilibrium during the play, we need to compute the range of κ (for the different combinations of games ϕ_A and ϕ_B) in which the two eigenvalues $\nu_1(p_i)$ and $\nu_2(p_i)$ are negative, conditional on the existence of the point (moving coordinates belonging to the unit square). Carrying this task systematically is not particularly difficult and all elements of the solution are defined analytically; however, its exposition is very complex due to the large amount of different cases to be considered. Rather than this, we turn to a more comprehensive and visual explanation of these results in the main text of the chapter.

Stability of the corner points $\{p_i\}_{i=1}^4$ can be explained in terms of the four critical values of kappa, $\{\kappa_n\}_{n=1}^4$, obtained in (3.21) and (3.23), in a simple manner. Taking p_1 as an example, one can compute directly that this point will be an attractor in the regions $R_1(p_1) = \big\{(\kappa, \phi_A, \phi_B) \in [0,1] \times [0,\pi] \times [0,\pi]\big\}$, $R_2(p_1) = \big\{(\kappa, \phi_A, \phi_B) \in [0, \kappa_2(\phi_A, \phi_B)] \times [0,\pi] \times [\pi, 2\pi]\big\}$, $R_3(p_1) = \big\{(\kappa, \phi_A, \phi_B) \in [k_2(\phi_A, \phi_B), 1] \times [\pi, 2\pi] \times [0,\pi]\big\}$, and that it is never stable in the region with $(\phi_A, \phi_B) \in [\pi, 2\pi] \times [\pi, 2\pi]$. Comparable partitions of the space of parameters can be computed for the other three points in a similar way.

Regarding the moving points (hybrid and mixed states), we enter into a richer situation where we have the existence condition given again by the four critical levels of κ that we already know, plus two additional values. The first new value,

$$\kappa_5(\phi_A, \phi_B) = \frac{\cos\phi_A + \sin\phi_A}{\cos\phi_A + \cos\phi_B + \sin\phi_A + \sin\phi_B}, \tag{3.26}$$

can be obtained from analyzing the sign of any of the two eigenvalues of the points $\{p_i\}_{i=5}^8$, or from $\nu_1(p_9)$. From the study of the sign of $\nu_2(p_9)$ we obtain

$$\kappa_6(\phi_A, \phi_B) = \frac{\cos\phi_A + \sin\phi_A}{\cos\phi_A - \cos\phi_B + \sin\phi_A - \sin\phi_B}. \tag{3.27}$$

This last critical value is usually less binding than κ_5 and plays a minor role in the analysis. As an illustration, the expression for $\nu_2(p_9)$ with $\phi_A = \phi_B = \arctan 2 - \pi$ (the angular parameters for the hawk-dove matrices (1.5) employed in Chapter 1) yields the negative and constant eigenvalue of $\nu_2(p_9) = -2/(3\sqrt{5})$. Multiplying by the corresponding scaling factor $\alpha_A = \alpha_B = 3\sqrt{5}$, we recover the value of -2 observed in the inset of Figure 1.2. See the main text in Section 3.4 for the final analysis of possible scenarios of the phase portrait.

Appendix B - Additional tables

Table 3.4: Bifurcation scenarios

Scenario	Π_A	Π_B	Region	Sequence of attractors
(1)	I	I	$\Phi_{\mathrm{I,I}}$	$\{p_i\}_{i=1}^4 \xrightarrow{\kappa_1} p_1, p_4$
(2)	I	II	$\Phi^+_{\mathrm{I,II}}$	$\{p_i\}_{i=1}^4 \xrightarrow{\kappa_4} p_1, p_2, p_3 \xrightarrow{\kappa_1} p_1$
		IV	$\Phi^-_{\mathrm{I,IV}}$	$\{p_i\}_{i=1}^4 \xrightarrow{\kappa_2} p_2, p_3, p_4 \xrightarrow{\kappa_3} p_4$
(3)	I	II	$\Phi^-_{\mathrm{I,II}}$	$\{p_i\}_{i=1}^4 \xrightarrow{\kappa_1} p_1, p_4 \xrightarrow{\kappa_4} p_1$
		IV	$\Phi^+_{\mathrm{I,IV}}$	$\{p_i\}_{i=1}^4 \xrightarrow{\kappa_3} p_1, p_4 \xrightarrow{\kappa_2} p_4$
(4)	I	III	$\Phi^+_{\mathrm{I,III}}$	$\{p_i\}_{i=1}^4 \xrightarrow{\kappa_2} p_2, p_3, p_4 \xrightarrow{\kappa_4} p_2, p_3$
			$\Phi^-_{\mathrm{I,III}}$	$\{p_i\}_{i=1}^4 \xrightarrow{\kappa_4} p_1, p_2, p_3 \xrightarrow{\kappa_2} p_2, p_3$
(5)	II	I	$\Phi_{\mathrm{II,I}}$	$p_1 \xrightarrow{\kappa_4} p_1, p_4$
	IV		$\Phi_{\mathrm{IV,I}}$	$p_4 \xrightarrow{\kappa_2} p_1, p_4$
(6)	II	II	$\Phi_{\mathrm{II,II}}$	p_1
	IV	IV	$\Phi_{\mathrm{IV,IV}}$	p_4
(7)	II	III	$\Phi^-_{\mathrm{II,III}}$	$p_1 \xrightarrow{\kappa_1} p_1, p_2, p_3 \xrightarrow{\kappa_2} p_2, p_3$
	IV		$\Phi^+_{\mathrm{IV,III}}$	$p_4 \xrightarrow{\kappa_3} p_2, p_3, p_4 \xrightarrow{\kappa_4} p_2, p_3$
(8)	II	III	$\Phi^0_{\mathrm{II,III}}$	$p_1 \xrightarrow{\kappa_2} p_5, p_7 \xrightarrow{\kappa_1} p_2, p_3$
	IV		$\Phi^0_{\mathrm{IV,III}}$	$p_4 \xrightarrow{\kappa_4} p_6, p_8 \xrightarrow{\kappa_3} p_2, p_3$
(9)	II	III	$\Phi^+_{\mathrm{II,III}}$	$p_1 \xrightarrow{\kappa_2} p_9 \xrightarrow{\kappa_5} p_5, p_7 \xrightarrow{\kappa_1} p_2, p_3$
	IV		$\Phi^-_{\mathrm{IV,III}}$	$p_4 \xrightarrow{\kappa_4} p_9 \xrightarrow{\kappa_5} p_6, p_8 \xrightarrow{\kappa_3} p_2, p_3$
(10)	III	I	$\Phi^+_{\mathrm{III,I}}$	$p_9 \xrightarrow{\kappa_2} p_1 \xrightarrow{\kappa_4} p_1, p_4$
			$\Phi^-_{\mathrm{III,I}}$	$p_9 \xrightarrow{\kappa_4} p_4 \xrightarrow{\kappa_2} p_1, p_4$
(11)	III	II	$\Phi^-_{\mathrm{III,II}}$	$p_9 \xrightarrow{\kappa_2} p_1$
		IV	$\Phi^+_{\mathrm{III,IV}}$	$p_9 \xrightarrow{\kappa_4} p_4$
(12)	III	II	$\Phi^+_{\mathrm{III,II}}$	$p_9 \xrightarrow{\kappa_5} p_5, p_7 \xrightarrow{\kappa_2} p_1$
		IV	$\Phi^-_{\mathrm{III,IV}}$	$p_9 \xrightarrow{\kappa_5} p_6, p_8 \xrightarrow{\kappa_4} p_4$
(13)	III	III	$\Phi^-_{\mathrm{III,III}}$	$p_9 \xrightarrow{\kappa_5} p_5, p_7 \xrightarrow{\kappa_1} p_2, p_3$
			$\Phi^+_{\mathrm{III,III}}$	$p_9 \xrightarrow{\kappa_5} p_6, p_8 \xrightarrow{\kappa_3} p_2, p_3$
(14)	VI	II	$\Phi^1_{\mathrm{IV,II}}$	$p_4 \xrightarrow{\kappa_3} p_2, p_3, p_4 \xrightarrow{\kappa_4} p_2, p_3 \xrightarrow{\kappa_2} p_1, p_2, p_3 \xrightarrow{\kappa_1} p_1$
	II	IV	$\Phi^1_{\mathrm{II,IV}}$	$p_1 \xrightarrow{\kappa_1} p_1, p_2, p_3 \xrightarrow{\kappa_2} p_2, p_3 \xrightarrow{\kappa_4} p_2, p_3, p_4 \xrightarrow{\kappa_3} p_4$
(15)	VI	II	$\Phi^2_{\mathrm{IV,II}}$	$p_4 \xrightarrow{\kappa_3} p_2, p_3, p_4 \xrightarrow{\kappa_2} \{p_i\}_{i=1}^4 \xrightarrow{\kappa_4} p_1, p_2, p_3 \xrightarrow{\kappa_1} p_1$
	II	IV	$\Phi^2_{\mathrm{II,IV}}$	$p_1 \xrightarrow{\kappa_1} p_1, p_2, p_3 \xrightarrow{\kappa_4} \{p_i\}_{i=1}^4 \xrightarrow{\kappa_2} p_2, p_3, p_4 \xrightarrow{\kappa_3} p_4$
(16)	VI	II	$\Phi^3_{\mathrm{IV,II}}$	$p_4 \xrightarrow{\kappa_2} p_1, p_4 \xrightarrow{\kappa_3} \{p_i\}_{i=1}^4 \xrightarrow{\kappa_1} p_1, p_4 \xrightarrow{\kappa_4} p_1$
	II	IV	$\Phi^3_{\mathrm{II,IV}}$	$p_1 \xrightarrow{\kappa_4} p_1, p_4 \xrightarrow{\kappa_1} \{p_i\}_{i=1}^4 \xrightarrow{\kappa_3} p_1, p_4 \xrightarrow{\kappa_2} p_4$
(17)	VI	II	$\Phi^4_{\mathrm{IV,II}}$	$p_4 \xrightarrow{\kappa_2} p_1, p_4 \xrightarrow{\kappa_4} p_1$
	II	IV	$\Phi^4_{\mathrm{II,IV}}$	$p_1 \xrightarrow{\kappa_4} p_1, p_4 \xrightarrow{\kappa_2} p_4$
(18)	VI	II	$\Phi^5_{\mathrm{IV,II}}$	$p_4 \xrightarrow{\kappa_4} p_9 \xrightarrow{\kappa_2} p_1$
	II	IV	$\Phi^5_{\mathrm{II,IV}}$	$p_1 \xrightarrow{\kappa_2} p_9 \xrightarrow{\kappa_4} p_4$
(19)	VI	II	$\Phi^6_{\mathrm{IV,II}}$	$p_4 \xrightarrow{\kappa_4} p_9 \xrightarrow{\kappa_5} p_5, p_7 \xrightarrow{\kappa_2} p_1$
	II	IV	$\Phi^6_{\mathrm{II,IV}}$	$p_1 \xrightarrow{\kappa_2} p_9 \xrightarrow{\kappa_5} p_6, p_8 \xrightarrow{\kappa_4} p_4$
(20)	VI	II	$\Phi^7_{\mathrm{IV,II}}$	$p_4 \xrightarrow{\kappa_4} p_9 \xrightarrow{\kappa_5} p_6, p_8 \xrightarrow{\kappa_3} p_2, p_3 \xrightarrow{\kappa_1} p_5, p_7 \xrightarrow{\kappa_2} p_1$
	II	IV	$\Phi^7_{\mathrm{II,IV}}$	$p_1 \xrightarrow{\kappa_2} p_9 \xrightarrow{\kappa_5} p_5, p_7 \xrightarrow{\kappa_1} p_2, p_3 \xrightarrow{\kappa_3} p_6, p_8 \xrightarrow{\kappa_4} p_4$
(21)	VI	II	$\Phi^8_{\mathrm{IV,II}}$	$p_4 \xrightarrow{\kappa_4} p_6, p_8 \xrightarrow{\kappa_3} p_2, p_3 \xrightarrow{\kappa_1} p_5, p_7 \xrightarrow{\kappa_2} p_1$
	II	IV	$\Phi^8_{\mathrm{II,IV}}$	$p_1 \xrightarrow{\kappa_2} p_5, p_7 \xrightarrow{\kappa_1} p_2, p_3 \xrightarrow{\kappa_3} p_6, p_8 \xrightarrow{\kappa_4} p_4$

TABLE 3.5: Angular values used in Figure 3.4.

Class I: $\phi \in (0, \frac{\pi}{2})$	Class II: $\phi \in (\frac{\pi}{2}, \pi)$	Class III: $\phi \in (\pi, \frac{3\pi}{2})$	Class IV: $\phi \in (\frac{3\pi}{2}, 2\pi)$
$\phi_1 = 0.414139$	$\phi_3 = 1.895701$	$\phi_9 = 3.364624$	$\phi_{14} = 4.913706$
$\phi_2 = 1.147486$	$\phi_4 = 2.074962$	$\phi_{10} = 3.785094$	$\phi_{15} = 5.005756$
	$\phi_5 = 2.498092$	$\phi_{11} = 4.154848$	$\phi_{16} = 5.167108$
	$\phi_6 = 2.628658$	$\phi_{12} = 4.199454$	$\phi_{17} = 5.269930$
	$\phi_7 = 2.848226$	$\phi_{13} = 4.511072$	$\phi_{18} = 5.779019$
	$\phi_8 = 2.940276$		$\phi_{19} = 5.989818$

TABLE 3.6: Payoff matrices used in Figure 3.5.

Class I: $\phi \in (0, \frac{\pi}{2})$	Class II: $\phi \in (\frac{\pi}{2}, \pi)$	Class III: $\phi \in (\pi, \frac{3\pi}{2})$	Class IV: $\phi \in (\frac{3\pi}{2}, 2\pi)$
$\Pi_1 = \begin{pmatrix} 20.3 & 5.1 \\ 11.2 & 9.1 \end{pmatrix}$	$\Pi_3 = \begin{pmatrix} 17.9 & 0 \\ 21.1 & 9.5 \end{pmatrix}$	$\Pi_9 = \begin{pmatrix} 2.2 & 21.7 \\ 11.9 & 19.5 \end{pmatrix}$	$\Pi_{14} = \begin{pmatrix} 6.9 & 19.6 \\ 4.9 & 9.8 \end{pmatrix}$
$\Pi_2 = \begin{pmatrix} 20.4 & 5.1 \\ 16.2 & 14.2 \end{pmatrix}$	$\Pi_4 = \begin{pmatrix} 14.6 & 0 \\ 19.4 & 8.8 \end{pmatrix}$	$\Pi_{10} = \begin{pmatrix} 0 & 20 \\ 8 & 14 \end{pmatrix}$	$\Pi_{15} = \begin{pmatrix} 7.7 & 19.2 \\ 4.8 & 9.6 \end{pmatrix}$
	$\Pi_5 = \begin{pmatrix} 12 & 0 \\ 20 & 6 \end{pmatrix}$	$\Pi_{11} = \begin{pmatrix} 2.1 & 21.2 \\ 7.4 & 12.7 \end{pmatrix}$	$\Pi_{16} = \begin{pmatrix} 9.4 & 19.9 \\ 5 & 10.9 \end{pmatrix}$
	$\Pi_6 = \begin{pmatrix} 10.7 & 0 \\ 19.4 & 4.9 \end{pmatrix}$	$\Pi_{12} = \begin{pmatrix} 0 & 19.4 \\ 4.9 & 10.7 \end{pmatrix}$	$\Pi_{17} = \begin{pmatrix} 10.6 & 21.2 \\ 5.3 & 12.7 \end{pmatrix}$
	$\Pi_7 = \begin{pmatrix} 9.6 & 0 \\ 19.2 & 2.9 \end{pmatrix}$	$\Pi_{13} = \begin{pmatrix} 2.9 & 19.6 \\ 4.9 & 9.8 \end{pmatrix}$	$\Pi_{18} = \begin{pmatrix} 8.8 & 19.4 \\ 0 & 13.6 \end{pmatrix}$
	$\Pi_8 = \begin{pmatrix} 9.8 & 0 \\ 19.6 & 2 \end{pmatrix}$		$\Pi_{19} = \begin{pmatrix} 9.6 & 19.2 \\ 0 & 16.3 \end{pmatrix}$

Conclusion

This thesis analyzes several aspects of evolutionary dynamics when the assumption of disjoint populations is relaxed. It makes two relevant contributions to the related literature: a conceptual one by making an exhaustive analysis of the model with coupled populations, and a methodological one by conducting an experiment in continuous time tailored to such a specific setup. The main conclusion is that one- and two-population models are robust with respect to moderate overlapping; but very rich structures can be observed in the transition regime between both cases which cannot be explained by any of the two models independently.

Chapter 1 introduced the fundamental idea with a model of coupled populations where both the intra- and the intergroup interactions were the same hawk-dove game. Human behavior in the lab is in good agreement with the hypotheses stated by replicator dynamics.

The next two chapters extended this study in two complementary directions. Chapter 2 dealt with the subtleties observed in the experimental data set, thus refining and complementing the analysis in Chapter 1. We considered deviations from the best response paradigm with the introduction of noise to explain the behavioral patterns.

Chapter 3 generalized the original model in order to allow for the intra- and intergroup interactions to be any pair of symmetric two-strategy games defined with 2×2 payoff matrices. With the introduction of an angular parametrization, the general model can be defined in terms of only three parameters: one characteristic of each game, and the coupling parameter; this simplifies the systematic analysis. There exist a maximum of twenty-one bifurcations that can be observed with replicator dynamics and these are expected to reduce to the order of four behavioral families with the introduction of noise in the best-response function.

Experimental instructions

Welcome to this experiment on economic decision making!

Please read these instructions carefully. The experiment is conducted anonymously. This means you will not get to know which of the other participants are interacting with you or which participant is acting in which role. Please note that you must not talk to other participants once the experiment has started. Also note that the use of mobile phones or similar devices is prohibited for the duration of the experiment. If you have any questions after reading these instructions, please raise your hand and we will come to your cubicle to answer your questions personally.

There are several peculiarities about this experiment:

- The experiment consists of six parts, but only one randomly selected part will be paid.
- You will play in multiple groups at the same time.
- The experiment is conducted in continuous time.

The different parts of the experiment

As mentioned above, there are six parts. At the end of the experiment, a random draw of the computer will determine which part is going to be paid. Please try to play each part as if it was the only one.

You will play in multiple groups at the same time

At the beginning of each part, the participants will be sorted into two groups.

This sorting is random and will take place anew at the beginning of each part. Thus, the composition of the groups will change in each part. That means that participants who were in your group in one part may be in the other group in the next part, and vice versa.

One of the two groups will consist of you and 11 other participants. This group is referred to as "your group" or "own group." The second group consists of 12 other participants and is referred to as the "other group."

You will always interact with both groups at the same time. The details on this interaction are discussed in a later section of these instructions. For now, just note that you (and all other participants) always need to choose between the options "A" and "B" and that your choice affects the interaction with both groups.

The experiment is conducted in continuous time

Each part lasts 210 seconds. At the beginning of a part, the computer will randomly select one of the options "A" or "B" for you to start with. After that, you can change your decision at any point in time and as often as you want. Below, you can see a screenshot of the experimental software. The left part of the screen informs you of the game that is played in the current part. This is also where you make your decision.

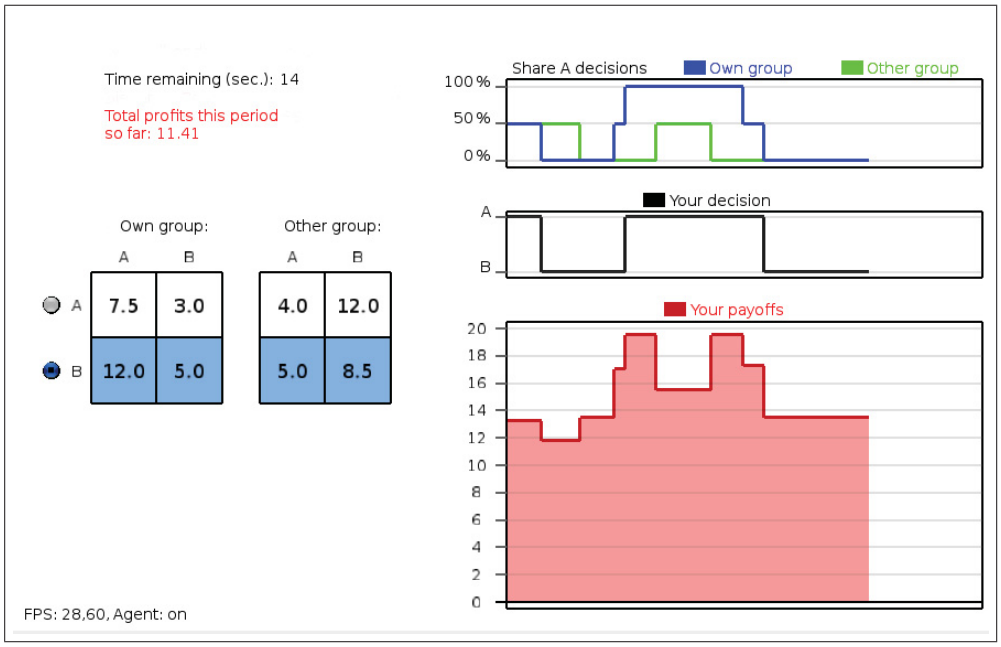

How do I make or change my decision?

The radio buttons on the far left of the screen determine your current choice. To change your decision, you can use the mouse to click on the corresponding radio button or you may also use the up and down keys on the keyboard to change your decision. The up key will select option "A" and the down key will select option "B." As previously mentioned, you can change your decision at any point in time during the entire part.

How can I see what the others are doing or what I did at an earlier point in time?

The decisions of participants are recorded and displayed in the upper-right area of the screen. The black line documents your own decisions over time. It depicts whether you chose "A" or "B" at a given point in time. The blue and the green line in the upper chart document the decisions of the participants in your own group and in the other group, respectively. Either line displays the share of participants who choose "A" in the corresponding group.

How do I see how much money I earn?

In this experiment, you earn a steady income that accumulates over time. The current income is documented in the red chart in the lower-right area of the screen. The higher the red line, the higher the income you earn. Note that your income is a flow of payoffs. If you realize an income of 10 for the entire duration of the part, you would earn a total payoff of 10 in that part. Analogously, an income of 15 means that you would receive 15 Euros if your income was constantly 15 and the corresponding part was randomly selected as the one chosen to be paid.

Your total profits are represented by the red area under the red line. Moreover, the red text in the upper-left area of the screen will always show the total payoffs you have realized so far.

How is my income calculated?

As mentioned above, you are always playing in two groups at the same time. The

interaction is described by two payoff matrices: the left matrix applies to the interaction with your own group, the right matrix describes the interaction with the other group. The matrices inform you of the income you can generate while playing with either group.

Consider the following example (from the screenshot):

	Your group		Other group	
	A	B	A	B
A	7.5	3.0	4.0	12.0
B	12.0	5.0	5.0	8.5

Assume you and all other participants (in both groups) choose "B." In this case, your income from your own group will be 5 (indicated in the lower-right corner of the left matrix) and your income from the other group would be 8.5. Your total income would thus be 13.5.

Another example, assume that one half of the participants in your group choose "A" while the other half of your group chooses "B." Moreover, assume that 70% of the participants in the other group choose "A" and that the remaining 80% choose "B."

- If you are among those who choose "A":
  Income from your group: $0.5 \times 7.5 + 0.5 \times 3 = 5.25$.
  Income from other group: $0.7 \times 4 + 0.3 \times 12 = 6.4$.
  Total income: $5.25 + 6.4 = 11.65$.

- If you are among those who choose "B":
  Income from your group: $0.5 \times 12 + 0.5 \times 5 = 8.5$.
  Income from with other group: $0.7 \times 5 + 0.3 \times 8.5 = 6.05$.
  Total income: $8.5 + 6.05 = 14.05$.

In general, the income streams are calculated as follows. The matrices below are general, *OwnPayXY* and *OthPayXY* are just placeholders for the entries of the matrix with your group and with the other group, respectively. The terms *OwnShareA*, *OwnShareB*, *OthShareA* and *OthShareB* represent the share of participants who choose "A" or "B" in either group, respectively.

	Your group		Other group	
	A	B	A	B
A	*OwnPayAA*	*OwnPayAB*	*OthPayAA*	*OthPayAB*
B	*OwnPayBA*	*OwnPayBB*	*OthPayBA*	*OthPayBB*

Your decision determines the relevant row of the payoff matrices. If you choose "A" only the first row is used, and if you choose "B" only the second row is used.

Your income from your group would be:

- If you choose "A":
  $OwnPayAA \times OwnShareA \ + \ OwnPayAB \times OwnShareB$
- If you choose "B":
  $OwnPayBA \times OwnShareA \ + \ OwnPayBB \times OwnShareB$

The same logic also applies to the interaction with the other group. Here, your income would be:

- If you choose "A":
  $OthPayAA \times OthShareA \ + \ OthPayAB \times OthShareB$
- If you choose "B":
  $OthPayBA \times OthShareA \ + \ OthPayBB \times OthShareB$

The only difference between the interactions with your own group and with the other group is that your own decision will have an impact on *OwnShareA* and *OwnShareB* but not on *OthShareA* and *OthShareB*.

Your total income is the sum of your income from your group and the income from the other group. Keep in mind that the red line will always show your current total income and that you may change your choice at any point in time. Moreover, the red text in the upper-left area of the screen will keep you informed of the payoffs you have accumulated so far.

Summary

- There are six parts. Only one randomly selected part will be paid in the end. Each part lasts 210 seconds.
- There are always two groups. The composition of these groups is random and will change in every part.
- You will play in two groups at a time: one with your own group and one with the other group.
- Both groups generate a flow of income and your actual payoff will accumulate over time.
- You can change your decision at any point in time. Use the radio buttons on the left side of the screen or the Up/Down keys on the keyboard to do so.

The experiment will start with three short (90 seconds) trial parts that will not affect your payoff. These are simply to familiarize you with the payoff structure and the software for this experiment.

If your have any further questions, please raise your hand and we will come to your cubicle to answer the questions personally.

Bibliography

Alós-Ferrer, C. and N. Netzer (2010). "The logit-response dynamics." *Games and Economic Behavior* 68, pp. 413–427.

Benndorf, V., I. Martínez-Martínez, and H.-T. Normann (2016). "Equilibrium selection with coupled populations in hawk-dove games: Theory and experiment in continuous time." *Journal of Economic Theory* 165, pp. 472–486.

Birch, L.C. (1957). "The meanings of competition." *The American Naturalist* 91.856, pp. 5–18.

Björnerstedt, J. and J.W. Weibull (1996). "Nash equilibrium and evolution by imitation." In: *The rational foundations of economic behavior*. Ed. by K.J. Arrow, E. Colombatto, M. Perlman, and C. Schmidt. London: Palgrave Macmillan.

Blanco, M., D. Engelmann, A.K. Koch, and H.-T. Normann (2010). "Belief elicitation in experiments: is there a hedging problem?" *Experimental Economics* 13.4, pp. 412–438.

– (2014). "Preferences and beliefs in a sequential social dilemma". *Games and Economic Behavior* 87, pp. 122–135.

Blume, L.E. (1993). "The statistical mechanics of strategic interaction." *Games and Economic Behavior* 5, pp. 387–424.

Brunner, C., C.F. Camerer, and J.K. Goeree (2011). "Stationary concepts for experimental 2×2 games: Comment". *The American Economic Review* 101, 1029–1040.

Camerer, C. and T.-H. Ho (1999). "Experience-weighted attraction learning in normal form games." *Econometrica* 67.4, pp. 827–874.

Cason, T.N., D. Friedman, and E. Hopkins (2014). "Cycles and instability in a Rock-Paper-Scissors population game: a continuous time experiment." *The Review of Economic Studies* 81, pp. 112–136.

Connell, J.H. and W.P. Sousa (1983). "On the evidence needed to judge ecological stability or persistence." *The American Naturalist* 121.6, pp. 789–824.

Cressman, R. (1995). "Evolutionary game theory with two groups of individuals." *Games and Economic Behavior* 11, pp. 237–253.

– (2003). *Evolutionary dynamics and extensive form games.* Cambridge, MA: MIT Press.

Denolf, J., I. Martínez-Martínez, H. Josephy, and A. Barque-Duran (in press). "A quantum-like model for complementarity of preferences and beliefs in dilemma games." *Journal of Mathematical Psychology.*

Friedman, D. (1991). "Evolutionary games in economics." *Econometrica* 59.3, pp. 637–666.

– (1996). "Equilibrium in evolutionary games: some experimental results." *The Economic Journal* 106.434, pp. 1–25.

Friedman, D. and B. Sinervo (2016). *Evolutionary games in natural, social, and virtual worlds.* New York, NY: Oxford University Press.

Goeree, J.K. and C.A. Holt (1999). "Stochastic game theory: For playing games, not just for doing theory." *Proceedings of the National Academy of Sciences USA* 96, pp. 10564–10567.

Goeree, J.K., C.A. Holt, and T.R. Palfrey (2005). "Regular Quantal Response Equilibrium." *Experimental Economics* 8.4, pp. 347–367.

Gómez-Gardeñes, J., C. Gracia-Lázaro, L.M. Floría, and Y. Moreno (2012). "Evolutionary dynamics on interdependent populations." *Physical Review E* 86.056113.

Greiner, B. (2015). "Subject pool recruitment procedures: organizing experiments with ORSEE." *The Journal of the Economics Science Association* 1, pp. 114–125.

Grimm, V. and F. Mengel (2014). "An experiment on learning in a multiple games environment." *The Journal of Economic Theory* 147.6, pp. 2220–2259.

Haile, P.A., A. Hortaçsu, and G. Kosenok (2008). "On the empirical content of quantal response equilibrium." *The American Economic Review* 98.1, pp. 180–200.

Harsanyi, J.C. and R. Selten (1988). *A general theory of equilibrium selection in games.* Cambridge, MA: MIT Press.

Hofbauer, J. and E. Hopkins (2005). "Learning in perturbed asymmetric games." *Games and Economic Behavior* 52, pp. 133–152.

Hofbauer, J. and W.H. Sandholm (2002). "On the Global Convergence of Stochastic Fictitious Play." *Econometrica* 70.6, pp. 2265–2294.

Hofbauer, J. and K. Sigmund (1998). *Evolutionary Games and Population Dynamics*. Cambridge, UK: Cambridge University Press.

– (2003). "Evolutionary game dynamics." *The Bulletin of the American Mathematical Society* 40.4, pp. 479–519.

Hopkins, E. (2002). "Two competing models of how people learn in games." *Econometrica* 70.6, pp. 2141–2166.

Huck, S., H.-T. Normann, and J. Oechssler (1999). "Learning in Cournot oligopoly–An experiment." *The Economic Journal* 109.454, pp. C80–C95.

Huck, S., P. Jehiel, and T. Rutter (2011). "Feedback spillover and analogy-based expectations: a multi-game experiment." *Games and Economic Behavior* 71.2, pp. 351–365.

Jehiel, P. (2005). "Analogy-based expectation equilibrium." *The Journal of Economic Theory* 123, pp. 81–104.

Kennedy, G.J.A. and C.D. Strange (1986). "The effects of intra- and inter-specific competition on the survival and growth of stocked juvenile Atlantic salmon, Salmo solar L., and resident trout, Salmo trutta L., in an upland stream." *The Journal of Fish Biology* 28.4, pp. 479–489.

Lambert-Mogiliansky, A. and I. Martínez-Martínez (2015). "Games with type indeterminate players". In: *Springer Lecture Notes in Computer Science*. Ed. by H. Atmanspacher et al. Vol. 8951. Springer International Publishing Switzerland, pp. 223–239.

Lieberman, E., C. Hauert, and M.A. Nowak (2005). "Evolutionary dynamics on graphs." *Nature* 433, pp. 312–326.

Lim, W. and P.R. Neary (2016). "An experimental investigation of stochastic adjustment dynamics." *Mimeo*.

Mailath, G.J. (1993). "Perpetual randomness in evolutionary economics." *Economics Letters* 42, pp. 291–299.

– (1998). "Do people play Nash equilibrium? Lessons from evolutionary game theory". *The Journal of Economic Literature* 36.3, pp. 1347–1374.

Martínez-Martínez, I. (2014). "A connection between quantum decision theory and quantum games: The Hamiltonian of Strategic Interaction." *Journal of Mathematical Psychology* 58, pp. 33–44.

Martínez-Martínez, I. and E. Sánchez-Burillo (2016). "Quantum stochastic walks on networks for decision-making." *Scientific Reports* 6.23812.

Mäs, M. and H.H. Nax (2016). "A behavioral study of "noise" in coordination games." *Journal of Economic Theory* 162, pp. 195–208.

Maynard Smith, J. (1982). *Evolution and the theory of games.* Cambridge, UK.: Cambridge University Press.

Maynard Smith, J. and G.R. Price (1973). "The logic of animal conflict." *Nature* 246.

McKelvey, R.D. and T.R. Palfrey (1995). "Quantal response equilibria for normal form games." *Games and Economic Behavior* 10, pp. 6–38.

Mengel, F. (2012). "Learning accross games." *Games and Economic Behavior* 74.2, pp. 601–619.

Nowak, M.A. and R.M. May (1992). "Evolutionary games and spatial chaos." *Nature* 359, pp. 826–829.

Oprea, R., K. Henwood, and D. Friedman (2011). "Separating the Hawks from the Doves: Evidence from continuous time laboratory games." *The Journal of Economic Theory* 146.6, pp. 2206–2225.

Page, K.M. and M.A. Nowak (2002). "Unifying evolutionary dynamics." *The Journal of Theoretical Biology* 219.1, pp. 93–98.

Pettit, J., D. Friedman, C. Kephart, and R. Oprea (2014). "Software for continuous game experiments." *Experimental Economics* 17, pp. 631–648.

Roll, R. (1994). "What every CFO should know about scientific progress in financial economics: what is known and what remains to be resolved." *Financial Management* 23.2, pp. 69–75.

Samuelson, L. (2001). "Analogies, adaptation, and anomalies." *The Journal of Economic Theory* 97.2, pp. 320–366.

Sandholm, W.H. (1998). "Simple and clever decision rules for a model of evolution." *Economics Letters* 61, pp. 165–170.

– (2010). *Population games and evolutionary dynamics.* Cambridge, MA: MIT Press.

Schoener, T.W. (1983). "Field experiments on interspecific competition." *The American Naturalist* 122.2, pp. 240–285.

Selten, R. (1980). "A note on evolutionarily stable strategies in asymmetric animal conflicts." *The Journal of Theoretical Biology* 84.1, pp. 93–101.

Selten, R. and T. Chmura (2008). "Stationary concepts for experimental 2×2 games." *The American Economic Review* 98.3, pp. 938–966.

Szabó, G. and G. Fáth (2007). "Evolutionary games on graphs." *Physics Reports* 446.4-6, pp. 97–216.

Taylor, C., D. Fudenberg, A. Sasaki, and M.A. Nowak (2004). "Evolutionary game dynamics in finite populations." *The Bulletin of Mathematical Biology* 66, pp. 1621–1644.

Taylor, P.D. and L.B. Jonker (1978). "Evolutionary stable strategies and game dynamics." *Mathematical Biosciences* 40.1-2, pp. 145–156.

Traulsen, A., D. Semmann, R.D. Sommerfeld, H.-J. Krambeck, and M. Milinski (2010). "Human strategy updating in evolutionary games." *Proceedings of the National Academy of Sciences USA* 107.7, pp. 2962–2966.

Weibull, J.W. (1995). *Evolutionary game theory*. Cambridge, MA: MIT Press.

Young, H.P. (2011). "Commentary: John Nash and evolutionary game theory." *Games and Economic Behavior* 71, pp. 12–13.

Zhuang, Q., Z. Di, and J. Wu (2014). "Stability of mixed-strategy-based iterative Logit Quantal Response dynamics in game theory." *PLOS ONE* 9.8, pp. 1–16.